Available online at www.sciencedirect.com
SCIENCE DIRECT®
Coordination Chemistry Reviews 244 (2003) 115–136
COORDINATION CHEMISTRY REVIEWS
www.elsevier.com/locate/ccr

Binary and ternary carbides of alkali and alkaline-earth metals

Uwe Ruschewitz *

Institut für Anorganische Chemie der Universität zu Köln, Greinstraße 6, 50939 Köln, Germany

Received 17 December 2002; accepted 30 March 2003

Contents

Abstract

The review surveys the preparation methods, crystallochemistry and physical properties (i.e. mainly spectroscopic properties) of binary and ternary carbides of Group I or Group II metals. Due to the low electronegativity of alkali and alkaline-earth metals the bonding in their binary carbides can be assumed to be ionic with carbon forming the anion. Therefore, the first part of this overview will be subdivided into chapters according to the type of the carbon anion, i.e. isolated C anions, C_2 and C_3 dumbbells. For the ternary carbides of alkali and alkaline-earth metals, which include an additional metal of other groups, the ionic description is not valid in all cases, as these compounds display interesting properties on the borderline between ionic and metallic behaviour.

Keywords: Alkali metals; Alkaline-earth metals; Carbides; Crystal structures; Physical properties; Synthesis

1. Introduction

Carbides are compounds that are formed by a metal or a semimetal and carbon, which possesses the higher electronegativity in these compounds. Depending upon the difference of the electronegativities (ΔE_N) of carbon and the metal/semimetal several classes of carbides are usually distinguished:

- salt-like carbides with high ΔE_N and ionic properties, e.g. CaC_2, Na_2C_2, Al_4C_3
- metallic carbides with intermediate ΔE_N and metallic properties, e.g. LaC_2, TiC, Fe_3C
- covalent carbides with small, almost vanishing ΔE_N and strong covalent bonding, e.g. SiC, B_4C.

This classification is, of course, very simple and especially the class of metallic carbides is not well-

* Tel.: +49-221-470-3285; fax: +49-221-470-4899.
E-mail address: uwe.ruschewitz@uni-koeln.de (U. Ruschewitz).

0010-8545/03/$ - see front matter
doi:10.1016/S0010-8545(03)00102-4

defined, as at least three different subclasses can be given depending upon their different properties:

- carbides of 4f and 5f elements containing C_2 dumbbells, e.g. LaC_2, Pu_2C_3, ThC_2
- interstitial carbides of the larger transition metals ($r_{metal} > 130$ pm) with simple crystal structures derived from close-packed metal atoms and C atoms occupying octahedral holes, e.g. Y_2C, TiC, W_2C
- a less well-defined group comprising metallic carbides not belonging to any of the other groups with $r_{metal} < 130$ pm and complicated crystal structures and complex, e.g. Cr_3C_2, Mn_5C_2, Fe_3C.

The situation will get even more complicated, if ternary carbides are included. The class of metallic carbides has already been reviewed in a few contributions emphasising the synthesis [1], structural [2–4] and/or electronic properties [5,6], not to mention several very informative and comprehensive textbook chapters [7]. Therefore, this review will restrict itself to the carbides of Group I and II, which belong to the class of salt-like carbides. This restriction excludes many interesting classes of compounds like borocarbides (e.g. CaB_2C_2 [8] and superconducting LnM_2B_2C with Ln = Lanthanide and M = Ni, Pd, Pt [9]) or mixed carbides halides (e.g. $Ca_3Cl_2C_3$ [10] and $Ln_2X_2C_2$ with X = Cl, Br, I [11]). Also intercalation compounds like KC_8 [12], fullerides like A_3C_{60} [13] and partly metallated hydrocarbons (e.g. $LiCH_3$ [14], NaC_2H [15–17] or $A_x[M^n(C_2H)_{x+n}]$ with A = alkali metal and M = transition metal [18]) will not be a part of this contribution.

According to the literature the class of salt-like carbides is further divided into three groups depending upon the anion carbon forms:

methanides with 'C^{4-}' anions, e.g. Be_2C, Al_4C_3
acetylides with 'C_2^{2-}' anions, e.g. Na_2C_2, CaC_2
allylenides with 'C_3^{4-}' anions, e.g. Li_4C_3, Mg_2C_3.

But taking this classification into account, to which class of compounds do Li_6C_6 [19] or Li_2C_4 [20] belong? Li_6C_6 is a permetallated benzene and Li_2C_4 a permetallated butadiyne, so they are usually classified as metallated hydrocarbons. But Na_2C_2, a 'typical' salt-like carbide, can also be considered as permetallated acetylene, which is a hydrocarbon as well. Also the argument that the synthesis of carbides and metallated hydrocarbons is quite different, does not hold for all compounds. Typical carbides like CaC_2 can be synthesised from the elements or the oxides and a surplus of carbon, whereas Li_6C_6 is synthesised from C_6Cl_6 and *tert*-butyllithium [19]. Alkali metal carbides A_2C_2 with A = Na–Cs are prepared from the metals solved in liquid ammonia, which are reacted with acetylene. Only Li_2C_2 is accessible by a direct combination of the elements. This little discussion shows that the distinction between salt-like carbides and permetallated hydrocarbons is not always clear-cut. Nevertheless, this review will only consider those salt-like carbides, which contain the 'typical' anions 'C^{4-}', 'C_2^{2-}', and 'C_3^{4-}', as previously used in the literature. The quotation marks shall indicate that especially the methanide anion 'C^{4-}' is only a formal description. The article will first present binary carbides of alkali and alkaline-earth metals classified by the different carbon anions. Emphasis is laid on their structural chemistry. Synthetic details and some of their physical properties will be described whenever necessary and possible. In a second part ternary carbides are introduced, which contain an alkali or alkaline-earth metal and another metal. Many of these compounds have been found just recently and they are therefore presented for the first time in a comprehensive form. Again structural aspects are to the fore, but synthetic details and physical properties will be given as well.

2. Binary alkali and alkaline-earth metal carbides

2.1. Binary alkali metal carbides

2.1.1. Alkali metal methanides

Li_4C, perlithiated methane, was first prepared by reaction of a large excess of lithium vapour with CCl_4 [21]. The resulting brittle grey–white solid is very sensitive to air and moisture. It was characterised by the products of hydrolysis with D_2O, which were analysed by mass spectroscopy. The yield of CD_4 based on CCl_4 was 10–18%. C_2D_4 (61%) and C_2D_2 (20%) were the main hydrolysis products pointing to Li_4C_2 and Li_2C_2 as the main products of the first reaction. In an improved synthesis the yield of CD_4 was increased to 40.5% (C_2D_2 58.5%) [22]. Later on it was shown that the reaction of lithium vapour with carbon vapour also leads to the formation of Li_4C [23]. But in this case the analysis of the hydrolysis products showed that Li_4C is only a minor product (0–10%), whereas Li_4C_3 is the principal product (40–65%). Work on the thermal stability of perlithiated hydrocarbons showed that Li_4C is the least stable compound, which transforms at 498 K to Li_4C_2, Li_4C_3, Li_2C_2, and elemental lithium [24]. The relative ratios of the possible products depend upon the temperature and the time of the pyrolysis experiments. At higher temperatures and reaction times longer than 10 min only Li_2C_2 is observed, which is the most stable compound of this series. To some extend Li_4C can be separated from elemental lithium [25], but no procedure was described to separate the perlithiated hydrocarbons from each other. Therefore no sample containing mainly Li_4C has been reported up to now. This purification problem and the insolubility in inert organic solvents hampered the structural characterisa-

tion of perlithiated hydrocarbons by X-ray powder and single-crystal analysis, respectively. Especially the structures of lithiated methanes attracted a lot of attention, as theoretical calculations had predicted that they should be excellent candidates for the observation of long sought *anti-Le Bel* and *Van't Hoff* simple planar carbon species [26]. But more recent calculations and experiments based on photoelectron spectroscopy of gas-phase species showed that CAl_3Si and CAl_3Ge are the first examples of neutral pentaatomic tetracoordinate planar carbon molecules [27].

The synthesis of alkali metal methanides of composition A_4C (A = Na–Cs) has not been described. Some information on Na_4C is given based on theoretical calculations [28].

2.1.2. Alkali metal acetylides

All alkali metal acetylides of composition A_2C_2 with A = Li–Cs are known. Their syntheses, crystal structures, and many of their physical and spectroscopic properties are well documented. The most general approach for the synthesis of alkali metal acetylides is the reaction of the alkali metals solved in liquid ammonia with acetylene:

$$2A(\text{liq. } NH_3) + 2C_2H_2 \overset{\text{liq. } NH_3}{\rightarrow} 2AC_2H + H_2$$

where A = Li–Cs [29–32].

After evaporating ammonia the colourless alkali metal hydrogen acetylides can be obtained in pure, polycrystalline form. Their crystal structures with the exception of LiC_2H are well-known [15–17,33], but they will not be described in this overview, as set out in the introductory chapter. LiC_2H already decomposes at the temperature of evaporating ammonia to form Li_2C_2 and C_2H_2 [34], therefore its crystal structure is only known with suitable stabilising donor molecules [35]. Na_2C_2 can be synthesised by heating NaC_2H in vacuum to temperatures of about 450 K [29,30]. For the heavier alkali metal acetylides however the heating must be performed in a surplus of the respective alkali metal at temperatures between 470 and 520 K [29,30].

$$2NaC_2H \overset{450\ K}{\rightarrow} Na_2C_2 + C_2H_2$$

$$2AC_2H + 2A \overset{470-520\ K}{\rightarrow} 2A_2C_2 + H_2 \quad A = K–Cs$$

Alkali metal acetylides A_2C_2 with A = Na–Cs can be obtained in a pure, polycrystalline form by the procedures described above, whereas the resulting Li_2C_2 exhibits a bad crystallinity as indicated by broad reflections in the X-ray powder patterns of the samples obtained in liquid ammonia [36]. Li_2C_2 in a highly crystalline form can be prepared by a direct combination of the elements [37,38]—Li_2C_2 is the only alkali metal carbide, which can be obtained from the elements. or by a reaction of coal with Li_2CO_3 in an electric arc furnace [39]. The latter leads to samples containing about 50% of Li_2C_2. Therefore only two synthetic procedures, in which lithium is reacted with graphite, give pure Li_2C_2 with good crystallinity. In the first synthesis lithium vapour is reacted with amorphous coal or graphite in a steel container at temperatures between 1073 and 1173 K [37]. The second procedure utilises an arc-melting furnace to combine lithium and graphite to form Li_2C_2 [38]. The reaction was complete after a few seconds, further heating only led to a decomposition of Li_2C_2.

The crystal structure of Li_2C_2 was first investigated by Secrist and Wisnyi, who found a monoclinic unit cell based on Weissenberg and rotation photographs and Debye–Scherrer X-ray powder patterns [40]. This unit cell has never been confirmed and the first complete structural solution of Li_2C_2 goes back to Juza et al. [37,41]. The unit cell was determined from rotation photographs and X-ray powder patterns. Li_2C_2 crystallises isotypic to Rb_2O_2 and Cs_2O_2 [42] (*Immm*, $Z = 2$). The crystal structure of Li_2C_2 is shown in Fig. 1, the C_2^{2-} dumbbells are aligned parallel to the *c* axis of the orthorhombic unit cell. A C–C distance of 120 pm was obtained as expected for a C–C triple bond [43].

Each Li atom is surrounded by six carbon atoms stemming from four different C_2 dumbbells with two of them co-ordinating *side-on* and two of them *end-on*. The C_2 dumbbells are placed in a eightfold co-ordination polyhedron. The crystal structure of Li_2C_2 can be described as a distorted *anti*-fluorite structure with the centres of gravity of the C_2 dumbbells occupying the Ca positions. Therefore it was attempted to find a phase transition to an undistorted *anti*-CaF_2 structure with disordered C_2 dumbbells at higher temperatures. In first experiments up to 623 K it was only found that the *a* axis and *b* axis increase with increasing temperature, whereas the *c* axis decreases [37]. This anisotropic thermal expansion behaviour is a very common phenomenon in acetylides, which is due to a librational

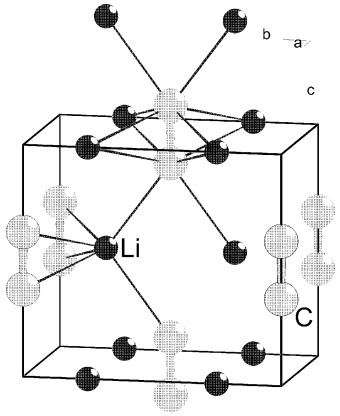

Fig. 1. Crystal structure of Li_2C_2 (*Immm*, $Z = 2$). The C–C triple bonds and the shortest contacts around one Li atom and a C_2 dumbbell are depicted.

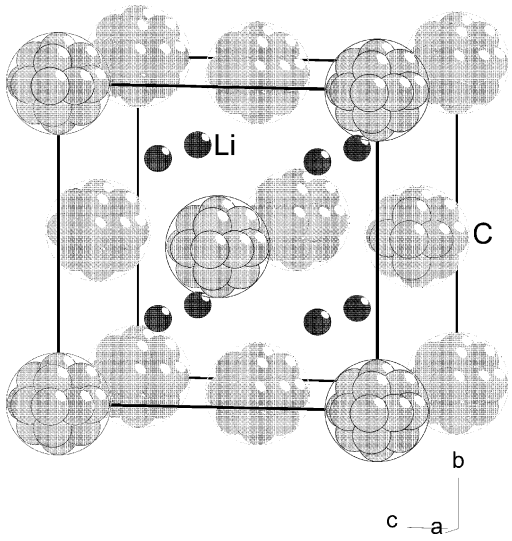

Fig. 2. Crystal structure of the high temperature modification of Li_2C_2 ($Fm\bar{3}m$, $Z = 4$). The disorder of the C_2 dumbbells is indicated (see text).

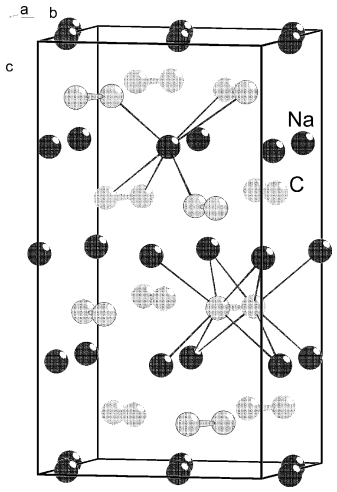

Fig. 3. Crystal structure of Na_2C_2 ($I4_1/acd$, $Z = 8$). The C–C triple bonds and the shortest contacts around one Na atom and a C_2 dumbbell are depicted.

motion of the C_2 units perpendicular to the dumbbell axis. In Li_2C_2 the C_2 dumbbells are aligned parallel to the c axis as already mentioned. Therefore this axis decreases slightly with increasing temperature. A phase transition of Li_2C_2 to an undistorted cubic *anti*-CaF_2 structure ($Fm\bar{3}m$, $Z = 4$) with disordered C_2 dumbbells was found in quite recent experiments at a temperature of about 693 K [38]. The resulting crystal structure is shown in Fig. 2. The disorder of the C_2 dumbbells is indicated in Fig. 2, but it must be mentioned that it is not known, whether this disorder is static or dynamic. This cannot be deduced from diffraction experiments. Solid state ^{13}C-NMR experiments, which are suitable for such investigations, have not been performed at temperatures above the transition temperature up to now. The phase transition between the high and the low temperature modifications of Li_2C_2 can be described by a group–subgroup scheme [44] with two *translationengleiche* transitions, as was shown in [38]. No further phase transitions of Li_2C_2—e.g. at temperatures below room temperature—have been observed up to now. It was found that the room temperature modification of Li_2C_2 (*Immm*, $Z = 2$) is also stable at 10 K [38]. Information on the spectroscopic properties of Li_2C_2 (Raman spectroscopy, solid state ^{13}C-NMR spectroscopy) will be given at the end of this chapter summarising the data for all alkali metal acetylides.

Na_2C_2 and K_2C_2 can be synthesised by the methods described above. They are obtained in an almost pure polycrystalline form. The samples should be colourless, but they are very often grey or even black because of minor amounts of carbon containing decomposition products, which are amorphous and cannot be seen in the X-ray powder patterns. Na_2C_2 and K_2C_2 crystallise in the same structure type. The first structural investigations on Na_2C_2 and K_2C_2 go back to Föppl, who found—based on X-ray powder investigations—that both compounds crystallise in a distorted *anti*-CaF_2 structure ($I4_1/acd$, $Z = 8$), which has not been observed in any other compound up to now [15]. In neutron diffraction experiments on Na_2C_2 a C–C distance of 120 pm was determined [45] confirming the expected value for a C–C triple bond. Later on a similar value for the C–C triple bond was found for K_2C_2 also based on neutron powder investigations [46]. The crystal structure of Na_2C_2 is shown in Fig. 3.

From Fig. 3 it can be seen that the C_2 dumbbells lie in the (0 0 1) plane perpendicular to the tetragonal c axis. Like in Li_2C_2 each Na atom is surrounded by six carbon atoms from four C_2 units, two of them co-ordinating *side-on* and two of them *end-on*. The C_2 dumbbells are co-ordinated by eight Na atoms. The crystal structure of Na_2C_2 (and K_2C_2) can be understood as another distorted variant of the *anti*-CaF_2 structure. It can also be obtained from the cubic CaF_2 structure by group–subgroup transitions. Three steps are necessary, one *translationengleiche* and two *klassengleiche* transitions. In the last *klassengleiche* transition the c axis has to be doubled. A phase transition from the room temperature structure to the undistorted cubic *anti*-fluorite structure ($Fm\bar{3}m$, $Z = 4$) was observed at about 570 K (Na_2C_2) and 423 K (K_2C_2), respectively [46]. This is shown in Fig. 4, which depicts the volumes of the low temperature modification (Na_2C_2 I) and high temperature modification of Na_2C_2 in dependence of the temperature as obtained from powder diffraction data using synchrotron radiation.

From Fig. 4 it is obvious that the phase transition from the room temperature modification of Na_2C_2 (Na_2C_2 I) to the high temperature modification (HT-Na_2C_2) is a first order transition. The resulting high

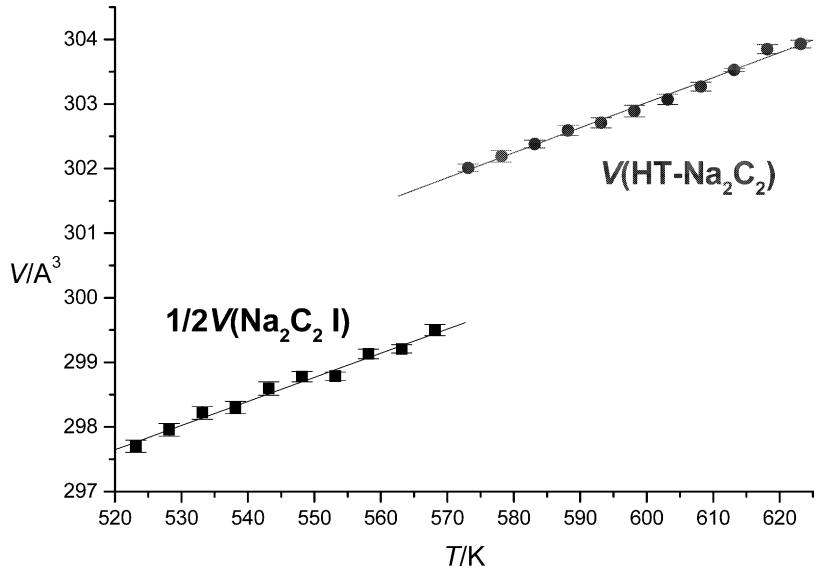

Fig. 4. Temperature dependence of the volume of low temperature Na_2C_2 I ($I4_1/acd$, $Z = 8$) and high temperature HT-Na_2C_2 ($Fm\bar{3}m$, $Z = 4$) as obtained from powder diffraction experiments using synchrotron radiation (powder diffractometer B2, Hasylab, Hamburg/Germany, $\lambda = 70.902$ pm) [47]. For comparison reasons the volume of Na_2C_2 I was divided by two.

temperature form of Na_2C_2 and K_2C_2 is isotypic to the high temperature modification of Li_2C_2 (see Fig. 2). Again no information is given about the disorder of the C_2 dumbbells, i.e. whether it is static or dynamic. This must be clarified by high temperature solid state NMR investigations. The reflection widths in the synchrotron powder investigations do not change significantly during the phase transitions of Na_2C_2 and K_2C_2, respectively [47]. DTA/TG measurements show that Na_2C_2 decomposes at about 900 K [47]. The mass loss of ca. 65% (Calc. 65.7%) between 923 and 1273 K points to a decomposition into carbon and sodium, which starts evaporating under these conditions. The boiling-point of sodium is observed at 1150 K, which is in good agreement with the literature data. No clear hint for a melting of Na_2C_2, as given in the literature [48], was found. Just recently a third modification of Na_2C_2 (Na_2C_2 II) was observed, which forms during the synthesis of Na_2C_2 from NaC_2H next to Na_2C_2 I at temperatures between 353 and 423 K in vacuum [49]. Heating in vacuum above 423 K leads to a complete transformation of Na_2C_2 II to Na_2C_2 I. This is shown in Fig. 5, which depicts the results of in situ X-ray powder diffraction measurements on the formation of Na_2C_2 from NaC_2H. Reaction mixtures obtained between 353 and 423 K contain both Na_2C_2 I and Na_2C_2 II after cooling to room temperature. The highest determined content of Na_2C_2 II was 31.7 wt.%. X-ray powder

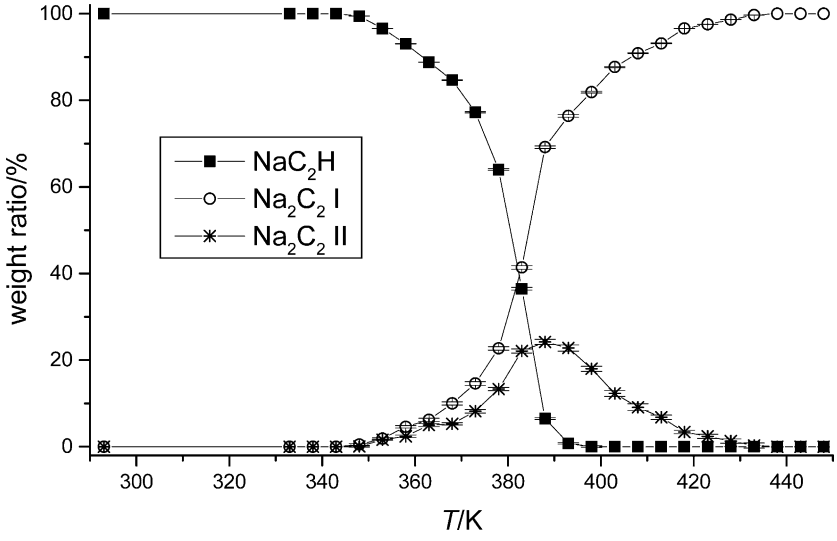

Fig. 5. In situ temperature dependent X-ray powder diffraction experiments on the formation of Na_2C_2 from NaC_2H in vacuum. The weight ratios of Na_2C_2 I, Na_2C_2 II, and NaC_2H are plotted as obtained from Rietveld refinements of the respective powder patterns.

investigations on this sample show that Na_2C_2 II is isotypic to the room temperature modification of Li_2C_2 (*Immm*, $Z = 2$, Rb_2O_2 structure type, see Fig. 1). Na_2C_2 II is likely to be a metastabile modification of Na_2C_2, but up to now there is no clear experimental evidence for this assumption [49]. No further modifications of Na_2C_2 and K_2C_2 were found at low temperatures down to 10 K [46]. Details of Raman and solid state NMR investigations on Na_2C_2 and K_2C_2 will be given at the end of this chapter.

The synthesis of Rb_2C_2 and Cs_2C_2 has been known for a long time [29–32], but no information about their crystal structures was available until recently [50]. The crystal structure analysis of Rb_2C_2 and Cs_2C_2 was hampered by the fact that no single crystals could be obtained and that two modifications coexist at room temperature. But by a combination of X-ray and neutron powder diffraction the crystal structures of both modifications were solved and refined. Rb_2C_2 as well as Cs_2C_2 crystallise in a hexagonal ($P\bar{6}2m$, $Z = 3$, Na_2O_2 structure type [42]) and an orthorhombic modification (*Pnma*, $Z = 4$, new structure type). As the reflections of both modifications overlap strongly, no reliable C–C distances were obtained from the refinements. They range between 50(10) and 139(1) pm with a clear trend of decreasing C–C distances with increasing temperatures [50]. A theoretical work based on density functional theory-based calculations [51] gave C–C distances between 125.4 and 126.0 pm thus confirming that the distances obtained in the experimental work are unreliable because of the experimental problems mentioned above. But still, the theoretical values for the C–C distances are longer by about 5 pm than the expected value for a C–C triple bond (120 pm). Therefore it would be worthwhile to reanalyse the crystal structures by using data of a high resolution neutron powder diffractometer such as the HRPD at the ISIS spallation facility.

The crystal structure of the hexagonal modification of Cs_2C_2 at 20 K is shown in Fig. 6. Hexagonal Cs_2C_2 is isotypic to Na_2O_2 [42] with two crystallographically distinct sites for the caesium and carbon atoms, respectively. Cs1 is co-ordinated by six carbon atoms with Cs–C distances less than 400 pm, four of them in an *end-on* and two in a *side-on* co-ordination. Cs2 on the other hand is co-ordinated by eight carbon atoms with Cs–C distances less than 400 pm, all of them in a *side-on* co-ordination. The two crystallographically distinct carbon atoms lead to two crystallographically distinct C_2 dumbbells, but both have a very similar co-ordination sphere of nine caesium atoms. The C–C distances obtained for this modification at 20 K are 93(5) pm (C1–C1) and 91(3) pm (C2–C2) and therefore much shorter than the expected value for a C–C triple bond (120 pm [43]). No hints for a phase transition were detected between 4 and 523 K, but a decrease of the hexagonal *c* axis between 4 and 300 K (the C_2 dumbbells are parallel to the *c* axis) and an increase of the *c* axis between 300 and 523 K with increasing temperature points to an interesting motion of the C_2 units in dependence of the temperature. Similar results were obtained for the hexagonal modification of Rb_2C_2, but here a low temperature modification was observed at temperatures of about 10 K, but its crystal structure is still unknown [50].

In Fig. 7 the crystal structure of the orthorhombic modification of Rb_2C_2 at room temperature is shown. It is a new structure type, but it is related to the *anti*-$PbCl_2$ structure type [52] with the centre of gravity of the C_2

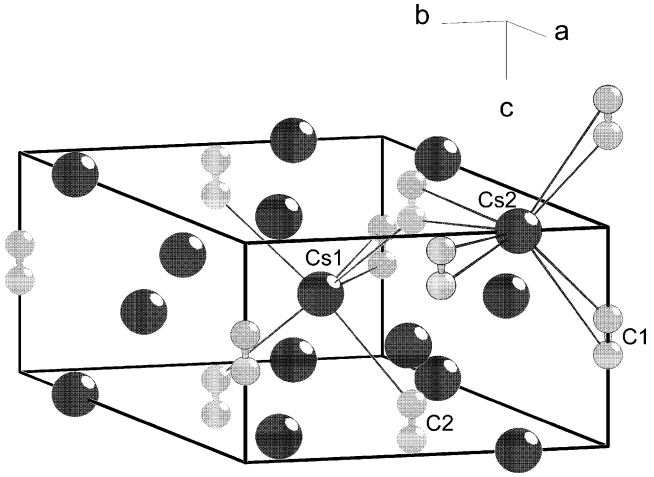

Fig. 6. Crystal structure of hexagonal Cs_2C_2 at 20 K ($P\bar{6}2m$, $Z = 3$). The C–C triple bonds and the shortest contacts (< 400 pm) around two crystallographically distinct caesium atoms are depicted.

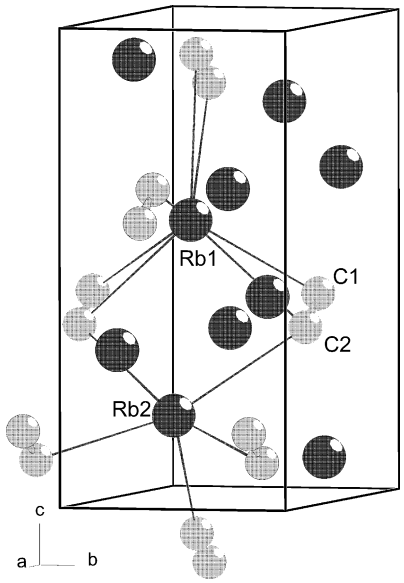

Fig. 7. Crystal structure of orthorhombic Rb_2C_2 at 298 K (*Pnma*, $Z = 4$). The C–C triple bonds and the shortest contacts (< 350 pm) around two crystallographically distinct rubidium atoms are depicted.

dumbbells occupying the Pb position. In the orthorhombic modification of Rb_2C_2 and Cs_2C_2 there are also two crystallographically distinct sites for the alkali metal and carbon atoms, respectively. Rb1 is co-ordinated by seven carbon atoms with Rb–C distances less than 350 pm, one of them in an *end-on* and six in a *side-on* co-ordination. Rb2 on the other hand is co-ordinated by five carbon atoms with Rb–C distances less than 350 pm, all of them in an *end-on* co-ordination. The co-ordination sphere is completed by two carbon atoms with a somewhat longer Rb–C distance of 387.1 pm. Similar co-ordinations were found for the orthorhombic modification of Cs_2C_2. In contrast to the hexagonal modification of Rb_2C_2 and Cs_2C_2 the two crystallographically distinct carbon atoms of the orthorhombic modification only lead to one crystallographically distinct C_2 dumbbell with a ninefold co-ordination polyhedron of the alkali metals. The C–C distance obtained for orthorhombic Rb_2C_2 at 298 K is 122.4(7) pm (C1–C2) and therefore in the range of the expected value for a C–C triple bond. No hints for a phase transition were detected between 4 and 573 K. Again a decrease of the orthorhombic *a* axis—the C_2 dumbbells lie in planes perpendicular to the orthorhombic *b* axis—with increasing temperature with two plateaux around 4 and 573 K points to an interesting motion of the C_2 units in dependence of the temperature. Investigations of this motion by solid state NMR experiments have not been reported up to now. There is no hint for a high or low temperature modification of orthorhombic Rb_2C_2 and Cs_2C_2 nor a transition between the orthorhombic and hexagonal modifications has been observed in dependence of the temperature. As both modifications coexist it remains unclear, which of both represents the thermodynamic stable modification. But from the theoretical investigations it was deduced that the orthorhombic modification is more stable by ≈ 7 kJ mol^{-1} (Rb_2C_2) and ≈ 4 kJ mol^{-1} (Cs_2C_2) in the athermal limit [51].

The orthorhombic and the hexagonal modifications of Rb_2C_2 and Cs_2C_2 show some similarities. The mean co-ordination number of the alkali metals is higher than in the crystal structures of Li_2C_2 and Na_2C_2/K_2C_2 (CN = 6). This can be directly correlated to the larger radii of Rb^+ and Cs^+, respectively. Furthermore the arrangement of the alkali metals in both modifications is similar, as can be seen in projections along [0 1 0] (orthorhombic modification) and [0 0 1] (hexagonal modification). The main difference is the orientation of the C_2 dumbbells, which lie in the projection plane of the orthorhombic modification, whereas they are perpendicular to the projection plane of the hexagonal modification. This difference is also displayed in the temperature dependence of the lattice parameters, as mentioned above.

Table 1
Raman spectroscopy: wave numbers of C–C stretching vibrations of binary alkali metal acetylides and acetylene

Compound	$\tilde{\nu}$(C≡C) (cm^{-1})
C_2H_2 [54]	1974
Li_2C_2 [38]	1872
Na_2C_2 [46]	1845
K_2C_2 [46]	1821
Rb_2C_2 [50]	1807 (orthorhombic) 1805 (hexagonal)
Cs_2C_2 [50]	1796 (orthorhombic/hexagonal)

Two ternary alkali metal acetylides $Na_xLi_{2-x}C_2$ ($x = 0.5$) and $KLiC_2$ are reported [53]. They can be obtained by a direct combination of the elements at about 1200 K. $Na_{0.5}Li_{1.5}C_2$ crystallises in a heavily disordered structure ($F\bar{4}3m$, $Z = 4$), which is related to the CaF_2 structure type. The crystal structure of $KLiC_2$ (*Pmmn*, $Z = 2$) however can be understood as a variant of the Li_2C_2 structure with half of the lithium sites replaced by potassium. The symmetry is therefore reduced: *Pmmn* is a direct subgroup of *Immm*, the space group of the crystal structure of Li_2C_2.

Raman spectroscopic investigations were performed on all binary alkali metal acetylides with emphasis of the stretching vibration of the C–C triple bond [38,46,50]. These results are summarised in Table 1.

From Table 1 it is obvious that there is a difference of more than 100 cm^{-1} between the wave number of the C–C stretching vibration in acetylene compared to those in binary alkali metal acetylides. This is usually interpreted in terms of the higher negative charge on the C_2 anions in the acetylides. This interpretation is further strengthened by the fact that the frequencies of the C–C stretching vibrations decrease with decreasing electronegativity of the alkali metal in the respective acetylides. A strong influence of packing effects can be ruled out, as the wave numbers of the C–C stretching vibration in

Table 2
Summary of solid-state ^{13}C-NMR spectroscopic data on binary alkali metal acetylides and acetylene

Compound	Technique	δ_{iso} [a] (ppm)	$\Delta\sigma$ [b] (ppm)	η [c]
Li_2C_2 [d]	Static [56]	195	375	0.18
Na_2C_2 [d]	Static [56]	170	358	0.14
	MAS [46]	172	342	0.17
K_2C_2	MAS [46]	186	285	0.15
C_2H_2	Static, CP [57]	70	240	0

[a] Relative to tetramethylsilane (TMS) $\delta_{iso} = -\sigma_{iso} = -1/3(\sigma_{11}+\sigma_{22}+\sigma_{33})$; $|\sigma_{33}-\sigma_{iso}| \geq |\sigma_{11}-\sigma_{iso}| \geq |\sigma_{22}-\sigma_{iso}|$.
[b] Anisotropy: $\Delta\sigma = \sigma_{33} - 1/2(\sigma_{11}+\sigma_{22})$.
[c] Asymmetry: $\eta = 3/2(\sigma_{22}-\sigma_{11})/\Delta\sigma$.
[d] $\Delta\sigma$ and η were calculated from the reported values for σ_{11}, σ_{22}, and σ_{33}.

different modifications of Rb_2C_2 and Cs_2C_2 with different C–Rb and C–Cs co-ordinations are almost the same. In alkali metal hydrogen acetylides with just one negative formal charge on the C_2H^- anion this trend of decreasing wave numbers of the C–C stretching vibration is less pronounced from NaC_2H (1871 cm^{-1}) to CsC_2H (1839 cm^{-1}), and the values of the wave numbers are larger than the wave numbers of the C–C stretching vibrations in the respective alkali metal acetylides A_2C_2 [33,55].

Furthermore some solid-state ^{13}C-NMR spectroscopic data based on static [56] and MAS measurements [46] are reported for Li_2C_2, Na_2C_2, and K_2C_2. The results of these measurements are summarised in Table 2.

In agreement with the results of the Raman spectroscopic investigations the isotropic chemical shift of alkali metal acetylides differs strongly from the value found for acetylene. The results of the static and MAS NMR measurements on Na_2C_2 are in good agreement, whereas the quality of the static spectrum obtained for Li_2C_2 only allows a rough determination of the anisotropic shielding parameters. Therefore a comparative discussion of these values for the three alkali metal acetylides is not possible. But it should be pointed out that all measurements give an asymmetry parameter $\eta \neq 0$. This is in agreement with their crystal structures, as the C_2 dumbbells do not have an axial symmetric co-ordination in these compounds and therefore the crystallographic axes perpendicular to the C–C bond differ.

2.1.3. Alkali metal allylenides

The allylenide anion C_3^{4-} is very rare in the chemistry of Group I and II carbides. Apart from Mg_2C_3 (Section 2.2.3) only Li_4C_3 has been synthesised and analysed. No allylenide of the higher alkali metals (Na–Cs) has been reported. Li_4C_3 was first prepared by the lithiation of propyne with *n*-butyllithium in hexane [58,59]. It was characterised by its polysilicon derivative tetrakis(trimethylsilyl)allene (**1**), which was obtained by reacting Li_4C_3 with trimethylchlorosilane in tetrahydrofuran.

$$H_3C\text{–}C{\equiv}CH + 4n\text{-}C_4H_9Li \rightarrow Li_4C_3 + 4C_4H_{10}$$
$$Li_4C_3 + 4Me_3SiCl \rightarrow (Me_3Si)_2C{=}C{=}C(SiMe_3)_2\ (\mathbf{1}) + 4LiCl$$

The allylenic structure of **1** could be deduced from its IR spectrum, which showed a signal at 1890 cm^{-1}, the typical region for an allylenic antisymmetric stretching vibration. A signal for an acetylenic stretching vibration is expected at approx. 2180 cm^{-1}. Solution NMR spectroscopy, mass spectroscopy and elemental analysis confirmed these findings. Li_4C_3, even in solution, reacts violently with water giving a gas identified as propyne with some allylene as minor product. No crystal structure analysis on Li_4C_3 is reported, neither on a single crystal or a crystalline powder. Our own experiments on the resulting highly reactive red solid show that it is amorphous to X-rays [60]. IR spectra of Li_4C_3 in hexane only show one absorption at 1675 cm^{-1} [59], which was interpreted as a strong indication that the allylenic form is also present in Li_4C_3. It is noteworthy that freshly prepared Li_4C_3 is soluble in hexane, but the precipitated Li_4C_3 cannot be redissolved in hexane anymore, even on warming [59]. This suggests that a structural change has taken place on precipitation. Later on it was shown that Li_4C_3 can also be synthesised by the reaction of Lithium vapour with carbon vapour (Section 2.1.1) [23] or by thermal treatment of Li_4C (Section 2.1.1) [24].

Interesting structures have been proposed for Li_4C_3 based on its IR spectra [61] or theoretical investigations [62] and it seems to be a quite important and interesting challenge to prepare and analyse crystalline samples of Li_4C_3.

2.2. Binary alkaline-earth metal carbides

2.2.1. Alkaline-earth metal methanides

Be_2C is the only alkaline-earth metal methanide, which was synthesised and structurally characterised. It has attracted some attention, as Be_2C seems to play an important role in the nuclear fusion reactor technology [63]. A polycrystalline sample containing about 94.7% Be_2C was obtained by the reaction of a slight surplus of BeO with sugar coal at about 2200 K in a hydrogen atmosphere [64,65]. Below 2070 K no reaction was observed and above 2370 K Be_2C starts decomposing. The red powder was purified by washing with hot diluted HCl pointing to the fact that the hydrolysis to methane and $Be(OH)_2$ is slow and the bonding in Be_2C is already quite covalent. Be_2C crystallises in the *anti*-CaF_2 structure type with $a = 433(1)$ pm and a Be–C distance of 187 pm, see Fig. 8 [66].

The electronic structure of Be_2C was calculated with linear-muffin-tin-orbital methods [67]. It is a semiconductor with an indirect band gap of approx. 1.2 eV. The

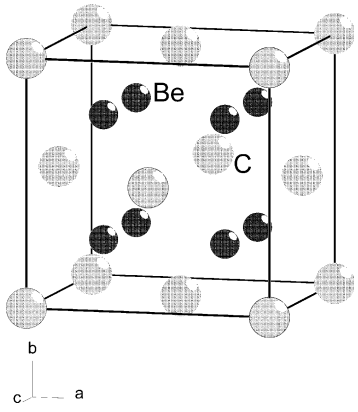

Fig. 8. Crystal structure of Be_2C ($Fm\bar{3}m$, $Z = 4$).

calculated lattice parameter a is somewhat smaller than the experimental value. In another theoretical work the electronic and structural properties of Be_2C and hypothetical Mg_2C in an *anti*-CaF_2 structure were calculated using first-principles pseudopotential total energy methods [68]. A similar indirect band gap was obtained for Be_2C (1.239 eV) and again, the calculated lattice parameter a is smaller ($a_{theor.} = 423$ pm) than the experimental value ($a_{exp.} = 433$ pm), but agrees well with the lattice parameter calculated from Pauling's tetrahedral covalent radii ($a_{Pauling} = 423$ pm). For Mg_2C a smaller indirect band gap was found (0.973 eV) and the theoretical value for the lattice parameter a agrees well with the value calculated from Pauling's covalent radii for a tetrahedral co-ordination ($a_{theor.} = 500$ pm; $a_{Pauling} = 501$ pm).

Calculations were also performed on the hypothetical Mg_2C molecule [69,70], but no theoretical and experimental information is given on methanides A_2C (A = Ca–Ba) of the heavier alkaline-earth metals.

2.2.2. Alkaline-earth metal acetylides

With the exception of BeC_2 the synthesis and structural properties of alkaline-earth metal acetylides are described in great detail. Especially for CaC_2 a large amount of literature is available due to its technical importance. Therefore this chapter will restrict itself on the most important facts of the synthesis of alkaline-earth metal acetylides, their crystal structures, and some of their physical properties, i.e. mainly spectroscopic properties.

The synthesis of BeC_2 from beryllium powder and acetylene at about 720 K was described by Durand [71]. After removing unreacted beryllium with boiling ether the successful synthesis of BeC_2 was proven by the evolution of acetylene after treatment of the resulting residue with water or hydrochloric acid. This synthesis was never repeated and no structural information on BeC_2 is available. Several publications dealt with the gas phase BeC_2 molecule. It was predicted that a triatomic ring structure should be the most stable structure [72]. The calculated bond lengths using different theoretical methods are in good agreement with those calculated in a very recent work. The C–C bond length was calculated to 126.6 pm, the Be–C bond length to 160.0 pm and the frequency of the C–C stretching vibration to 1809 cm^{-1} [73].

MgC_2 was first obtained by Novák in 1910 by the reaction of magnesium with acetylene [74]. It was found that the reaction starts at about 720 K, but at 770 K MgC_2 already starts decomposing into Mg_2C_3 and carbon. As acetylene is unstable under these conditions, the carbide was always contaminated by polymerised organics and carbon black. Furthermore MgO was formed, as magnesium reacts efficiently with any oxygen impurity in the surrounding atmosphere. No samples containing more than 56 wt.% of MgC_2 were obtained by different approaches [75–79]. A soxhlet extraction with a diethyl ether–ethyl bromide solution resulted in samples containing about 70 wt.% MgC_2 [77], but the crystallinity of the carbide was decreased by this procedure. A tetragonal unit cell was already determined in one of the earliest investigations [77], but surprisingly the complete structural arrangement remained unknown until 1998, when independently two groups were able to solve the crystal structure of MgC_2 [80,81]. In the first publication [80] the crystallinity and purity of the sample was increased by adding iodine to the magnesium powder prior to the reaction with acetylene. A sample containing about 75 wt.% of highly crystalline MgC_2 was obtained, the crystal structure was solved from X-ray powder diffraction data. In the second publication [81] a sample containing about 40 wt.% MgC_2 was investigated, but the use of neutron powder diffraction data led to very reliable structural results. The crystal structure of MgC_2 is shown in Fig. 9.

As expected from earlier results of hydrolysis experiments, which led to the evolution of acetylene [77,79], the crystal structure of MgC_2 contains C_2 dumbbells with a C–C distance of 121.5(7) pm [81]. This value is only slightly longer than the expected value for a C–C triple bond (120 pm [43]). The crystal structure of MgC_2 represents a variant of the tetragonal structure of CaC_2 (CaC_2I), in which the C_2 dumbbells are aligned parallel to the tetragonal c axis (see below). Here, the C_2 dumbbells lie in a plane perpendicular to the tetragonal c axis. Thus, the crystal structure of MgC_2 shows some similarities with the ThC_2 structure type [82]. Magnesium has a 2+4+4 co-ordination (217.4 pm 2 ×, 258.3 pm 4 ×, 284.7 pm 4 ×), whereas the co-ordination of calcium in CaC_2I can be described as a 2+8 co-ordination (see below). It must be assumed that the different sizes of the metal ions are responsible for this structural change. Both structures—MgC_2 and CaC_2(I)—can be understood as variants of the NaCl

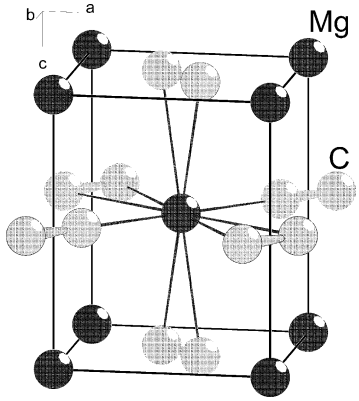

Fig. 9. Crystal structure of MgC_2 ($P4_2/mnm$, $Z = 2$). The C–C triple bonds and the shortest contacts (< 285 pm) around one magnesium atom are depicted.

structure type with ordered C_2 dumbbells. Their space-groups—$P4_2/mnm$ and $I4/mmm$, respectively—are connected to $Fm\bar{3}m$, the space group of NaCl, by group–subgroup relations. For CaC_2I a phase transition to a cubic structure with disordered C_2 dumbbells is observed (see below), whereas MgC_2 decomposes to Mg_2C_3 and carbon at about 770 K [77–79], before a phase transition can be observed. The decomposition is exothermic and Mg_2C_3 will be described in more detail in Section 2.2.3. Theoretical investigations were performed on the MgC_2 gas phase molecule [83,84], which found a primarily ionic bonding. In both publications a T-shaped cluster with a *side-on* co-ordination of magnesium was calculated as the stable structure, the calculated Mg–C distances are ca. 10–15 pm shorter than the Mg–C distances found in the solid state structure with a linear arrangement. In the more recent work [84] also a $(MgC_2)_4$ tetramer was investigated, in which the C_2^{2-} anion is co-ordinated *side-on* and *end-on* by Mg^{2+}, which is comparable to what is seen in transition metal metcar compounds (metallocarbohedrenes). The calculated Mg–C distances are well within the range found for the solid state structure.

CaC_2 was prepared for the first time in 1890 by the reaction of calcium oxide or carbonate with carbon and magnesium [85,86]. A few years later, it was shown that CaC_2 can also be synthesised in an electrical arc by reacting calcium oxide or carbonate with sugar coal [87–89]. In the first structural investigation a body centered tetragonal unit cell was found [90,91], and it was followed that calcium carbide crystallises in a distorted rock-salt structure with C_2-dumbbells aligned along the tetragonal c axis. This was confirmed later on by neutron powder and more recently by X-ray single-crystal diffraction experiments [92,93]. The crystal structure of the tetragonal room temperature modification of CaC_2, named CaC_2I, is shown in Fig. 10.

It is a well-known structure with all C_2 dumbbells aligned parallel to the tetragonal c axis. From neutron powder diffraction and X-ray single-crystal investigations a C–C distance of 120(1) pm and 120(2) pm was obtained [92,93], which is exactly the value expected for a C–C triple bond [43]. Calcium has a 2+8 co-ordination (259.6 pm 2×, 281.3 pm 8×). As already mentioned, CaC_2I and MgC_2 are distorted variants of the NaCl structure type. Thus, the metals form a distorted fcc arrangement, the octahedral holes are occupied by C_2 dumbbells. The crystal structures of MgC_2 and CaC_2I therefore only differ in the arrangement of the C_2 dumbbells: in CaC_2I they are all parallel to the tetragonal c axis, whereas in MgC_2 the C_2 dumbbells are parallel to the face diagonal of the (0 0 1) plane and the direction of this orientation is turned by 90° between two adjacent layers. Franck et al. [94,75] and, in more detail, Bredig [95] investigated the phase diagram of CaC_2. Aside from the tetragonal room-temperature modification CaC_2I, they found a cubic high-temperature modification CaC_2IV, a low-temperature modification CaC_2II, and a fourth modification CaC_2III, which was assumed to be metastabile. CaC_2IV can be described as a rock-salt structure with disordered C_2-dumbbells [96,97]. As for alkali metal acetylides A_2C_2 (A = Li, Na, K; see Section 2.1.2) it is not known, whether this disorder is static or dynamic. The crystal structure of CaC_2IV is shown in Fig. 11. The phase transition from CaC_2I to CaC_2IV occurs at about 763 K and is a first-order transition, as could be concluded from a volume jump in the $V=f(T)$ curve [98].

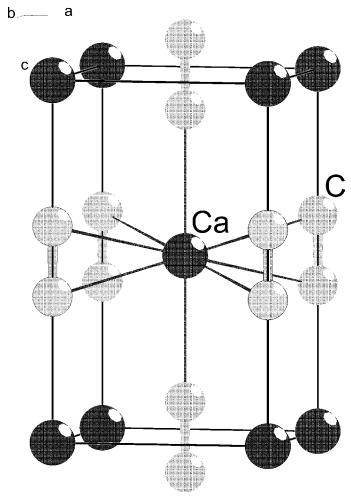

Fig. 10. Crystal structure of tetragonal CaC_2 (CaC_2I; $I4/mmm$, $Z=2$). The C–C triple bonds and the shortest contacts (< 290 pm) around one calcium atom are depicted.

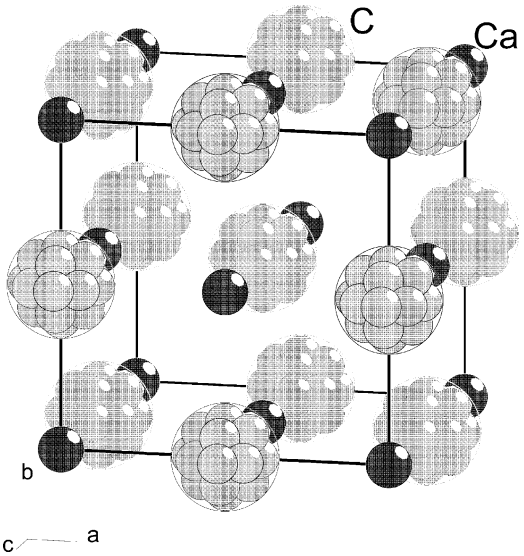

Fig. 11. Crystal structure of cubic high temperature modification CaC_2IV ($Fm\bar{3}m$, $Z=4$). The disorder of the C_2 dumbbells is depicted as a static disorder on several carbon positions (see text).

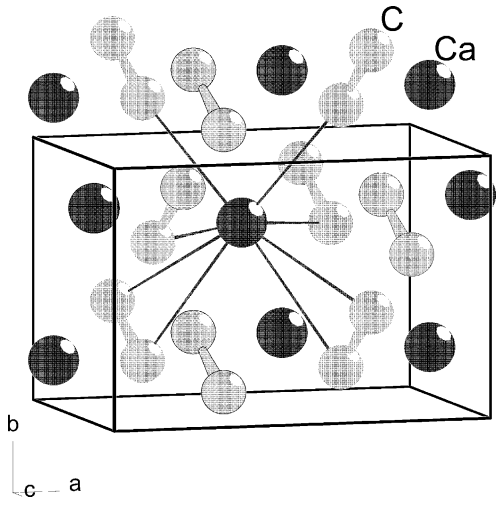

Fig. 12. Crystal structure of low-temperature CaC_2II ($C2/c$, $Z=4$). The C–C triple bonds and the shortest contacts (<290 pm) around one calcium atom are depicted.

The crystal structures of CaC_2II and CaC_2III were investigated by means of single-crystal X-ray diffraction [97,99]. On the assumption that CaC_2II and CaC_2III were changed by mistake in these publications, low-temperature modification II was refined in space group $B2_1/c$ ($Z=8$) and metastabile modification III in space group $C\bar{1}$ ($Z=8$). But careful examination of these results showed [80,98] that CaC_2(II) can be described in space group $C2/c$ and is isotypic to ThC_2 [82]. This structure is shown in Fig. 12. Again the calcium ions form a distorted fcc arrangement and the C_2 dumbbells occupy octahedral holes. But the orientation of the dumbbells now leads to a monoclinically distorted structure. The refinement of the crystal structure from synchrotron powder diffraction data (83 K) gave a C–C distance of 118.7(9) pm and eight Ca–C distances between 258.1(5) and 281.6(5) pm [98].

A close inspection of the X-ray single-crystal data published on metastabile CaC_2III [99] suggested that a twinned crystal was investigated as several unusual

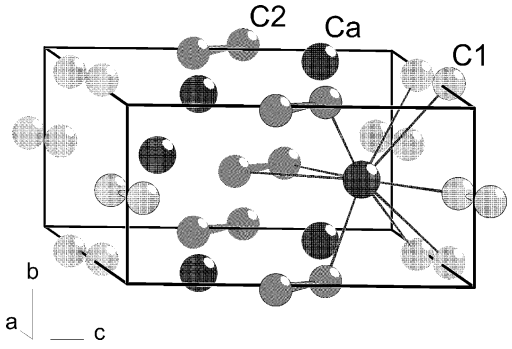

Fig. 13. Crystal structure of metastabile CaC_2III ($C2/m$, $Z=4$). The C–C triple bonds and the shortest contacts (<295 pm) around one calcium atom are shown. Crystallographically distinct carbon atoms are depicted in different colours.

reflection extinctions can be found in the published F_o/F_c list. This is further confirmed by the fact that a powder pattern calculated from the resulting crystal structure is not in agreement with the original data [75]. Therefore the crystal structure of metastabile CaC_2III could be solved just recently on the basis of synchrotron powder data [98]. The sample under investigation contained three modifications of CaC_2 (I, II, III), but still the crystal structure of metastabile CaC_2III was determined unambiguously. This was confirmed by ^{13}C-MAS-NMR experiments, as the two crystallographically distinct positions of the carbon atoms in CaC_2III led to a splitting of the NMR signals [100]. For the NMR investigation a sample containing pure CaC_2III was used, which was prepared from CaC_2I and CaC_2II by a cyclic heating and cooling procedure in the temperature interval 310–790 K. The crystal structure of CaC_2III is shown in Fig. 13. The two crystallographically distinct carbon atoms are depicted in different colours. The refinement of the crystal structure from synchrotron powder diffraction data (83 K) gave C–C distances of 127(4) and 118(3) pm, nine Ca–C distances between 242(2) and 292(1) pm were found [98]. The resulting distances should be considered with some care, as the sample under investigation contained three CaC_2 modifications. It is very likely that CaC_2III is a metastabile modification at 295 K, as it exhibits the smallest density ($\rho_{calc}=2.1712(3)$ g cm^{-3}), whereas CaC_2I has the highest density ($\rho_{calc}=2.2026(1)$ g cm^{-3}; CaC_2II: $\rho_{calc}=2.1798(2)$ g cm^{-3}) [98].

It is known that the existence of different modifications of CaC_2 is highly dependent upon impurities like oxygen, nitrogen, sulphur, or an excess of calcium [101]. Therefore in the latest publications a synthesis from calcium (purified by distillation) and carbon (heated to 1070 K in vacuum prior to the reaction) in a purified atmosphere and using inert reaction vessels was used [93,98,100]. But still no clear picture of the stability ranges of each modification could be given, probably due to the fact that particle size and thermal treatment of the sample also have a strong influence on their formation. Therefore, the phase diagram given by Bredig is still valid [95] and for an improved picture more detailed investigations are necessary. But at ambient temperature it was found that in technical CaC_2 the ratio of tetragonal CaC_2I is higher than in pure CaC_2 prepared from the elements. In the latter low-temperature modification CaC_2II dominates [98]. However, performing the synthesis from the elements with an excess of calcium mainly tetragonal CaC_2I is formed [100]. It is surprising that the "simple' binary system CaC_2 shows such a complicated behaviour.

It is interesting to compare the structural properties of CaC_2 with the results of theoretical calculations using extended Hückel [102] and Hartree-Fock methods [103]. In both calculations the structure with the C_2 dumbbells

aligned parallel to the *c* axis, i.e. pointing towards the corner of the Ca_6 octahedron, is lowest in energy, thus CaC_2I should be the most stable structure. But the extended Hückel calculations showed that small distortions with the C_2 dumbbells pointing towards the faces or the edges of the Ca_6 octahedra have very low-energy barriers [102]. And in fact, the distortion in CaC_2II is very small (tilt angle $\alpha = 12.8^\circ$), so that a phase transition from CaC_2I to CaC_2II is comprehensible. In CaC_2III the tilting of the $(C1)_2$ dumbbell is even smaller ($\alpha = 4.7^\circ$), but the tilting of the second, crystallographically distinct $(C2)_2$ dumbbell is very large ($\alpha = 39.9^\circ$). This might be a reasonable explanation for the metastabile character of CaC_2III. On the basis of Hartree-Fock calculations a slightly different picture was obtained, as the resulting energy barrier for distortions from the undistorted CaC_2I structure was calculated to be much higher [103]. Therefore it was concluded that in contradiction to the structural investigations distorted low temperature modifications should not be realised.

SrC_2 was synthesised for the first time by Moissan by reacting $Sr(OH)_2$ or $SrCO_3$ with sugar coal in an electrical arc furnace [88,104,105]. The first crystallographic investigations using a polycrystalline sample were reported by von Stackelberg [90]. He showed that at ambient temperature SrC_2 crystallises in the tetragonal CaC_2(I) structure (see Fig. 10). This was confirmed later on by X-ray single-crystal investigations [93]. Temperature-dependent X-ray powder diffraction data showed that at about 643 K a phase transition to a cubic high temperature modification occurs, which is analogous to CaC_2IV (see Fig. 11) [75,94,95]. Investigations using pure SrC_2 prepared from the elements resulted in a transition temperature of 700 K, from a volume jump in the $V = f(T)$ curve a first order transition could be concluded [106]. The higher transition temperature of the later experiment confirms the influence of impurities on phase transitions. Furthermore a low temperature modification of SrC_2 was found, which was assumed to be isotypic to CaC_2II (ThC_2 structure type, see Fig. 12) [75,94,95]. This was confirmed by Rietveld refinement of X-ray powder diffraction data [106], but even at 10 K no complete transition from tetragonal room temperature SrC_2 (SrC_2 I) to monoclinic low temperature SrC_2 (SrC_2 II) was observed. The transition temperature and the ratio SrC_2 I:SrC_2 II seem to depend highly on the crystal size of the sample. In this respect it is interesting to note that X-ray single-crystal investigations on SrC_2 at 210 K also resulted in the tetragonal SrC_2 I structure [93]. All phase transitions of SrC_2 were shown to be reversible and no metastabile modification analogous to CaC_2III was observed.

The results on BaC_2 are comparable to those obtained for SrC_2. The first synthesis of BaC_2 was performed by reacting BaO or $BaCO_3$ with magnesium and carbon [86], 2 years later a successful preparation in an electrical arc furnace from BaO or $BaCO_3$ and sugar coal was reported [88,107]. Again, the first structural investigations go back to von Stackelberg, who found a tetragonal unit cell and assumed a crystal structure isotypic to CaC_2I (see Fig. 10) [90]. Temperature-dependent X-ray powder investigations revealed a high temperature modification BaC_2IV (isotypic to CaC_2IV, see Fig. 11) [75,94,95] with a transition temperature of 423 K. In a more recent publication [108] a transition temperature of 523 K (first order transition) was determined for a sample prepared from the elements. In this work also a low temperature modification BaC_2II could be detected and refined using neutron powder diffraction data (isotypic to ThC_2/CaC_2II, see Fig. 12). Again a strong influence of the particle size on the phase transition was found. Furthermore a single crystal of BaC_2 was obtained by reacting $BaCO_3$ and graphite in an electrical arc. The X-ray analysis confirmed the BaC_2I structure with a C–C bond length of 118.6(13) pm. Using neutron powder diffraction data a C–C bond length of 118.5(3) pm was obtained for a sample prepared from the elements. It is interesting to note that the neutron powder diffraction data give a more accurate C–C distance than the X-ray data, although a single crystal was analysed. A notable aspect of the single-crystal X-ray analysis is the fact that the anisotropic thermal ellipsoids have their largest elongation perpendicular to the C–C bond indicative for a librational motion of the C_2 dumbbells around their centre of gravity. This is confirmed by the temperature dependence of the lattice parameters, as the *c* axis decreases with increasing temperature, whereas the *a* axis increases. It is therefore surprising that the single crystal investigations on CaC_2 and SrC_2 gave thermal ellipsoids with their longest elongation along the direction of the C–C bond [93].

Raman spectroscopic investigations were performed on CaC_2, SrC_2, and BaC_2 with emphasis on the stretching vibration of the C–C triple bond. For MgC_2 no signal for the C–C stretching vibration could be obtained [109]. The results are summarised in Table 3.

The values of the C–C stretching vibrations of alkaline-earth acetylides are very similar to the values found for alkali metal acetylides (see Table 1) and differ by more than 100 cm^{-1} from the value found for acetylene. As for the alkali metal acetylides the frequencies decrease with an increasing atomic number probably due to the decreasing electronegativity. Different wave numbers were found for the different modifications of CaC_2, whereas for the different modifications of Rb_2C_2 and Cs_2C_2 (see above) the same wave number of the C–C stretching vibration was observed.

Solid-state ^{13}C-NMR spectroscopic data based on static and MAS measurements were reported for all

Table 3
Raman spectroscopy: wave numbers of C–C stretching vibrations of binary alkaline-earth metal acetylides

Compound	$\tilde{\nu}$(C≡C) (cm^{-1})
CaC_2I [93]	1860
CaC_2II [93]	1871
SrC_2 [106]	1852
BaC_2 [110]	1831

known alkaline-earth metal acetylides. The results of these measurements are summarised in Table 4.

Our unpublished results on MgC_2 are included in Table 4. They have to be considered with some care, as amorphous carbon impurities lead to a broad, very strong signal around 125 ppm (typical for aromatic carbon), but the chemical shielding parameters obtained for MgC_2 fit nicely into the trend observed for the other alkaline-earth metal acetylides. In agreement with the results of the Raman spectroscopic investigations (Tables 1 and 3) the isotropic chemical shifts of alkaline-earth metal acetylides and of alkali metal acetylides differ strongly from the value obtained for acetylene (Table 2). The isotropic chemical shift δ_{iso} generally increases—i.e. the chemical shielding decreases—with an increasing atomic number. Therefore Li_2C_2 seems to be an exception. It might be interesting to repeat the measurements on Li_2C_2 using the MAS technique, although the results given in Table 4 show that the isotropic chemical shifts obtained from MAS spectra differ only slightly from those obtained from static measurements. The trend for $\Delta\sigma$ is less obvious, but $\Delta\sigma$ seems to decrease with an increasing atomic number. This can be seen for the alkali metal acetylides (Table 2) and the alkaline-earth metal acetylides (Table 4). Many ^{13}C-NMR spectra of CaC_2 were taken, but in most examples it was not clear, which of the three known at room temperature stable modifications was really measured. Only in the most recent publication [100] it was possible to measure single-phase products. It is a beautiful result of this work that two signals for the two crystallographically distinct carbon atoms of CaC_2III were detected, thus confirming the crystal structure solved from powder diffraction data. In another work on CaC_2 [112] also two signals were found, which differ strongly in their intensities. It was assumed that they belong to two different modifications of CaC_2. This seems plausible according to the data given in Table 4. Still not understood are the values for the asymmetry η. In modification AC_2I (A = Ca, Sr, Ba) they should be zero, as the C_2 dumbbells have an axial symmetric coordination according to their crystal structures. It is obvious from Table 4 that the deviations from $\eta = 0$ are large. The η values are even larger than those obtained for alkali metal acetylides, where according to the crystal structures $\eta \neq 0$ is expected. Several explanations were given for this unexpected behaviour. So it was assumed that in AC_2I the C_2 dumbbells are only statistically aligned along the tetragonal c axis [112]. In this respect the results obtained for the pure modifications of CaC_2 are intriguing [100]: the asymmetry parameters are very similar for all three modifications under investigation, i.e. the local symmetry seems to be quite comparable, although from their crystal structures a different picture is obtained. Meyer et al. [100] also gave the halfwidths of the NMR signals. They are largest for CaC_2I and smaller for CaC_2II and CaC_2III. This was interpreted in terms that the signal for the C_2 dumbbells in CaC_2I is a convolution of differently orientated C_2 units. Thus the large deviation of η from zero would be explained, but it is still not clear that the single-crystal analysis on CaC_2I did not give any hint for such a disorder [93].

2.2.3. Alkaline-earth metal allylenides

Mg_2C_3 is the only known alkaline-earth metal allylenide. Its synthesis from magnesium and different hydrocarbons (e.g. n-pentane or methane) at about 970 K was described [74]. It was also known since that time that above 970 K Mg_2C_3 decomposes to Mg and amorphous carbon and that MgC_2 decomposes to Mg_2C_3 and carbon at about 770 K:

$$2MgC_2 \overset{770\ K}{\rightarrow} Mg_2C_3 + C$$

$$Mg_2C_3 \overset{970\ K}{\rightarrow} 2Mg + 3C$$

The latter reaction was investigated in detail. From kinetic data using *Arrhenius*' equation an activation energy $E_A = 333$ kJ mol^{-1} was obtained [113]. Furthermore a thermal stability of Mg_2C_3 at 6 GPa up to 1720 K was found. From hydrolysis experiments, which gave mainly propyne and propadiene, it was concluded that the crystal structure of Mg_2C_3 must contain C_3^{4-} units [114,115]. The evolution of C3 hydrocarbons on hydrolysis and the opportunity to synthesise Mg_2C_3 from magnesium and methane attracted some interest from industrial chemists, as this could be an easy way to convert methane into higher hydrocarbons containing reactive C–C double or triple bonds. In two patents the synthesis of Mg_2C_3 from MgO and methane at about 1670 K was described [116,117]. Due to the thermal instability of Mg_2C_3 the reaction mixture has to be quenched rapidly to 970 K or less. The resulting mixture of propadiene and propyne after hydrolysis was reacted with a dehydrocyclisation catalyst to form benzene. The resulting by-product of the hydrolysis $Mg(OH)_2$ can be converted to MgO, which is recycled into the process. In another patent [118] the mixture of propyne and propadiene after hydrolysing Mg_2C_3 was reacted in the presence of an ion-exchanged Y zeolite catalyst composited with a Group VIB or Group VIII metal forming

trimethylbenzene. It should be mentioned that these patents were released without knowing the crystal structure of Mg_2C_3. The latter was not known until 1992, when based on X-ray and neutron powder diffraction data the crystal structure of Mg_2C_3 was solved and refined [119]. The resulting structural arrangement is shown in Fig. 14. Since $a:b:c \approx \sqrt{3}:\sqrt{2}:1$ of the orthorhombic unit cell, a hexagonal unit cell was given for a long time [77], which probably hampered the structural solution for a long time.

The crystal structure of Mg_2C_3 contains linear $C{=}C{=}C^{4-}$ units, which are isoelectronic with CO_2. The resulting C–C distance of 133.2(2) pm is slightly longer than that obtained for propadiene (131 pm [120]). As can be seen in Fig. 14 magnesium is co-ordinated by five carbon atoms of four C_3 dumbbells, three of them *end-on* (220.5, 222.4 pm 2 ×) and two of them *side-on* (231.7, 245.9 pm) with the magnesium atom sitting above the double bond similar to a π-complex. The carbon atoms show a quite different co-ordination. The negatively charged terminal carbon atom C2 of the C_3 group is co-ordinated to the magnesium atoms in a manner similar to that found in salt-like alkaline-earth metal acetylides. The central carbon atom C1 formally with no charge is only co-ordinated to two magnesium atoms. The resulting Mg–C distances are similar to those found for MgC_2 (217.4 pm 2 ×, 258.3 pm 4 ×). Mg_2C_3 is the only structurally characterised example of a carbide containing exclusively C_3 carbon groups. In Sc_3C_4 C_3 groups are found next to C_1 and C_2 groups [121]. The hydrolysis of Mg_2C_3 and Sc_3C_4 was compared in a detailed study [122]. In agreement with the crystal structure and former investigations the hydrolysis of Mg_2C_3 yields a mixture of propyne and propadiene, the ratio of which is close to equilibrium values at ambient temperature and shifts towards propadiene at low temperatures. Therefore it must be assumed that propadiene is the main hydrolysis product, which is converted to thermodynamically stable propyne under reaction conditions. Metallic $Sc_3C_4 \equiv Sc^{III}_{15}(C)_6(C_2)(C_3)_4(e^-)_3$ however forms upon hydrolysis a complex mixture of different hydrocarbons and hydrogen, as found for many other metallic carbides. No vibrational and ^{13}C-NMR spectroscopic investigations are published on Mg_2C_3.

Table 4
Summary of solid-state ^{13}C-NMR spectroscopic data on binary alkaline-earth metal acetylides

Compound	Techniques	δ_{iso} [a] (ppm)	$\Delta\sigma$ [b] (ppm)	η [c]
MgC_2	MAS [111]	167	330	0.0
CaC_2 (technical)[d]	MAS [93]	207	325	0.30
CaC_2[d]	MAS [93]	199	325	0.33
CaC_2I[d]	MAS [100]	199	325	0.34
CaC_2II[d]	MAS [100]	198	315	0.40
CaC_2III[d]	MAS [100]	204/197	303/279	0.38/0.28
CaC_2	MAS [112]	206.2 (200.3)	331	0.31
CaC_2[d]	Static [56]	200	345	0
SrC_2[d]	MAS [93]	213	322	0.03
SrC_2[d]	Static [56]	212	319	0
BaC_2[d]	MAS [93]	231	266	0.07
BaC_2	MAS [112]	232.1	265	0.38
BaC_2[d]	Static [56]	229	270	0

[a] Relative to tetramethylsilane (TMS) $\delta_{iso} = -\sigma_{iso} = -1/3(\sigma_{11}+\sigma_{22}+\sigma_{33})$; $|\sigma_{33}-\sigma_{iso}| \geq |\sigma_{11}-\sigma_{iso}| \geq |\sigma_{22}-\sigma_{iso}|$.
[b] Anisotropy: $\Delta\sigma = \sigma_{33} - 1/2(\sigma_{11}+\sigma_{22})$.
[c] Asymmetry: $\eta = 3/2(\sigma_{22}-\sigma_{11})/\Delta\sigma$.
[d] $\Delta\sigma$ and η were calculated from the reported values for σ_{11}, σ_{22}, and σ_{33}.

3. Ternary alkali and alkaline-earth metal carbides

3.1. Ternary alkali metal carbides

$KAgC_2$, the first ternary alkali metal carbide (i.e. acetylide), has been known since 1963 [123]. It was synthesised from KC_2H and highly explosive Ag_2C_2 in liquid ammonia:

$$2KC_2H + Ag_2C_2 \xrightarrow{\text{liq. } NH_3} K[Ag(C_2H)_2] + KAgC_2$$

By decreasing the KC_2H:Ag_2C_2 ratio almost pure $KAgC_2$ was available. Its existence was confirmed by elemental analysis. A symmetric structure around the C_2 unit was assumed, as no signal was found for the C–C stretching vibration in the IR spectra. Only in 1999 its crystal structure was solved by means of X-ray and neutron powder diffraction data [124]. The crystal structure is shown in Fig. 15. The modified synthesis avoided the use of explosive Ag_2C_2 by a slightly different approach:

$$2KC_2H + AgI \xrightarrow{\text{liq. } NH_3} K[Ag(C_2H)_2] + KI$$

$$K[Ag(C_2H)_2] \xrightarrow{400\ ^\circ C} KAgC_2 + C_2H_2$$

Using this or slightly modified approaches many ternary transitions metal acetylides of composition AM^IC_2 with A = Li–Cs and M^I = Cu [125], Ag [124], Au [126] were synthesised.

The crystal structure of $KAgC_2$ (Fig. 15) is characterised by $^1_\infty[Ag(C_2)^-_{2/2}]$ chains running parallel to the tetragonal *c* axis. These chains are separated by the potassium ions, which co-ordinate to four C_2 dumbbells in a *side-on* fashion. The crystal structure of $LiAgC_2$ is shown in Fig. 16. Again $^1_\infty[Ag(C_2)^-_{2/2}]$ chains are the characteristic structural motif, but now a hexagonal unit cell is found and the smaller lithium ions only co-ordinate *side-on* to three C_2 dumbbells.

In $CsAgC_2$ (see Fig. 17) $^1_\infty[Ag(C_2)^-_{2/2}]$ chains do not run parallel to each other, but they are arranged in layers perpendicular to the *c* axis, and the layers are

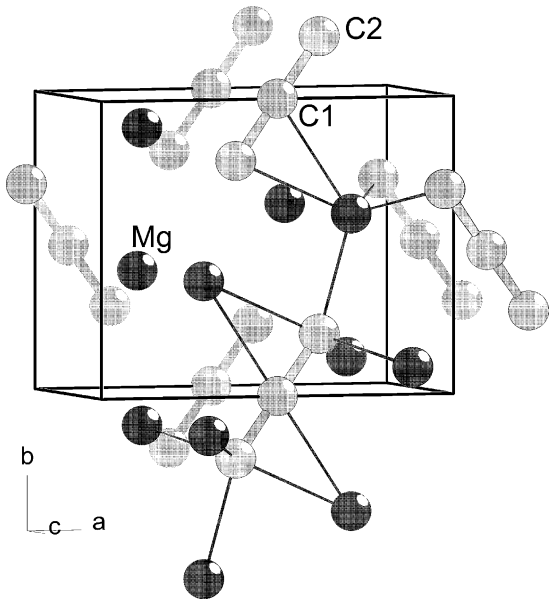

Fig. 14. Crystal structure of Mg_2C_3 (*Pnnm*, $Z = 2$). The C–C bonds and the shortest contacts (< 250 pm) around one magnesium atom and one C_3 dumbbell are shown.

rotated by 90° to each other. Thus, the caesium ions are co-ordinated pseudo-tetrahedrally by four C_2 dumbbells. The three different structure types found for $LiAgC_2$, $KAgC_2$, and $CsAgC_2$ correspond to the three simplest rod packings as given by O'Keeffe and Andersson [127]. The $^1_\infty[Ag(C_2)^-_{2/2}]$ chains can be assumed as rods and the alkali metal ions occupy the holes in-between. The structural changes from $LiAgC_2$ to $CsAgC_2$ were explained on the basis of a simple model of close packed rods ($^1_\infty[Ag(C_2)^-_{2/2}]$ chains) and spheres (alkali metal ions) [126]. All known alkali metal transition metal acetylides of composition AM^ICu_2 (A = Li-Cs; M^I = Cu, Ag, Au) crystallise in one of the three structure types given above. This is shown in Table 5.

Several aspects are obvious from Table 5. $RbCuC_2$ and $CsAgC_2$ show polymorphic behaviour, as two modifications were identified in the powder patterns at room temperature. Furthermore the high standard deviations of the lattice parameters of ternary gold acetylides are notable. They are due to a severe anisotropic peak broadening, which was found in all compounds crystallising in the $LiAgC_2$ or $KAgC_2$ structure type, but the strongest effect was found for gold acetylides. The anisotropic peak broadening displays the anisotropic structural features of compounds crystallising in the $LiAgC_2$ or $KAgC_2$ structure type, where the transition metal carbon chains run parallel to the *c* axis. (0 0 l) reflections are sharp, whereas all other reflections are severely broadened. Compounds crystallising in the $CsAgC_2$ structure type, where the chains are not running parallel to one axis, do not show this effect. Another interesting aspect of the lattice parameters given in Table 5 is a comparison of the lengths of the axes, which are parallel to the transition metal carbon chains, i.e. *c* axis in $LiAgC_2$ and $KAgC_2$ structure types and *a* axis in $CsAgC_2$ structure type. It is conspicuous that these axes, which are the sum of two M^I–C and one C–C bond lengths and almost independent of the respective alkali metal ions, are longer by more than 10 pm in all silver compounds compared to the respective gold compounds. This can be attributed to relativistic effects. It was predicted that this effects should be most obvious in the pair Ag–Au [128].

Based on neutron powder diffraction experiments a C–C bond length of 122.3(6) and 121.7(7) pm was found for $KAgC_2$ and $CsAgC_2$, respectively [124]. These values are only slightly longer than the expected value for a C–C triple bond (120 pm [43]). All ternary transition metal acetylides of composition AM^ICu_2 (A = Li–Cs) are either colourless (M^I = Cu, Ag) or yellow (M^I = Au). They are electronic insulators, as determined by conductivity measurements and confirmed by band structure calculations [124]. $KCuC_2$, $RbCuC_2$, and $CsCuC_2$ show intriguing ^{13}C-MAS-NMR spectra [125], as the carbon resonance line is complicatedly split due to the coupling of the carbon nucleus ($I = 1/2$) with the copper nuclei ($I = 3/2$ for the isotopes ^{63}Cu and ^{65}Cu). Additionally, the dipolar interaction between the copper nuclei has to be considered. Only a few examples for these effects in ^{13}C-Cu pairs have been seen before [129,130]. The Raman spectroscopic properties of compounds of composition AM^ICu_2 (A = Li–Cs; M^I = Cu, Ag, Au) will be discussed together with the Raman spectroscopic results on compounds of composition A_2MC_2 (A = Na–Cs; M = Pd, Pt) later on.

Ternary acetylides of composition A_2MC_2 (A = Na–Cs; M = Pd, Pt) are synthesised by a solid state reaction of the respective alkali metal acetylide A_2C_2 with palladium or platinum [131–133]. The reaction starts at about 410 K and must be performed in inert atmosphere due to the sensitivity of binary alkali metal acetylides and products to air and moisture. It is also possible to perform the synthesis in a glass capillary and to follow the reaction by means of X-ray powder diffraction. This was used to get some information on the kinetics of these solid state reactions [134]. The resulting compounds are black powders, their crystal structures were solved and refined from X-ray and neutron powder diffraction data. All compounds of composition A_2MC_2 (A = Na–Cs; M = Pd, Pt) crystallise in the same structure, which is shown in Fig. 18. The resulting lattice parameters are given in Table 6.

The crystal structure of compounds of composition A_2MC_2 (A = Na–Cs; M = Pd, Pt) is characterised by $^1_\infty[M(C_2)^{2-}_{2/2}]$ chains, which are separated by the alkali metal ions. The co-ordination sphere of the latter is somewhat unexpected, as it is formed by three carbon atoms and three palladium or platinum atoms. The

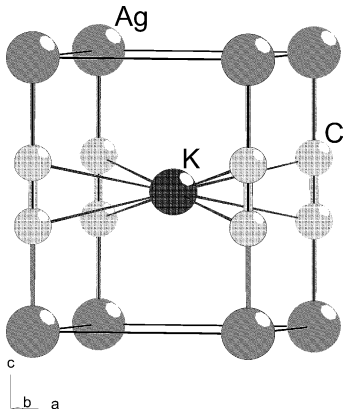

Fig. 15. Crystal structure of $KAgC_2$ ($P4/mmm$, $Z=1$). The C–C bonds, Ag–C bonds, and the co-ordination of the potassium atom are shown.

alkali metal–Pd(Pt) distances are slightly longer than the alkali metal–C distances.

The powder diffraction patterns of compounds of composition A_2MC_2 do not show any significant reflection broadening as was found for compounds of composition AM^IC_2. Therefore, very reliable lattice parameters were obtained, which show again a significant longer c axis for the compounds of the 4d element, i.e. palladium. The difference is approx. 6 pm and thus significantly smaller than the difference found for $AAgC_2$ and $AAuC_2$ compounds. This is in agreement with the theory, which predicts the strongest relativistic effects for the pair Ag–Au [128].

Neutron powder diffraction investigations were performed on Na_2PdC_2 and Na_2PtC_2 [132]. The resulting C–C bond lengths are 126.3(3) and 128.9(4) pm, respectively. These values are distinctively longer than the value expected for a C–C triple bond (120 pm [43]) and lie somewhere in-between a C–C triple and double bond (133.4 pm [43]). This was put down to a strong backbonding from the metals into the antibonding orbitals of the C_2 units, which should weaken the C–C bond and increase the bond length [132]. Band structure calculations and Raman spectroscopic investigations confirmed this assumption. The results of the Raman spectroscopic investigations are given in Table 7. For comparison reasons the results obtained for compounds of composition AM^IC_2 (A = Li–Cs; M^I = Cu, Ag, Au) are also given.

It is obvious from Table 7 that the wave numbers of the C–C stretching vibrations of ternary acetylides of composition A_2MC_2 are smaller by more than 100 cm^{-1} than the respective wave numbers in ternary acetylides of composition AM^IC_2. This corresponds to the C–C bond lengths as obtained from neutron powder diffraction data: Na_2PdC_2 126.3(3) pm; Na_2PtC_2 128.9(4) pm; $KAgC_2$ 122.3(6) pm; $CsAgC_2$ 121.7(7) pm.

Conductivity measurements and band structure calculations showed that ternary alkali metal transition metal acetylides of composition A_2MC_2 are semiconductors with a small indirect band gap (ca. 0.1–0.2 eV [132]). This corresponds to their black colour. Measurements of the magnetic susceptibilities revealed a diamagnetic behaviour as expected for Pd(0) and Pt(0) compounds. In Table 8 the results of solid-state ^{13}C-MAS-NMR investigations on ternary acetylides of composition A_2MC_2 are summarised.

Only for Na_2PdC_2 and K_2PdC_2 NMR spectra were obtained that allowed a reliable determination of the shielding parameters. For Na_2PtC_2 and K_2PtC_2 only the isotropic chemical shift was determined. The values for δ_{iso}, $\Delta\sigma$, and η are in the ranges obtained for binary alkali metal and alkaline-earth metal acetylides, but differ very much from the values obtained for acetylene (see above). Also the trends for δ_{iso}, $\Delta\sigma$, and η in dependence of the respective alkali metal are similar to those in the binary compounds, but less pronounced. An asymmetry parameter $\eta > 0$ is consistent with the lack of axial symmetry around the C_2 dumbbells in the crystal structures of ternary palladium and platinum acetylides.

An intermediate product of the synthesis of $NaCuC_2$ from NaC_2H and CuI in liquid ammonia is $NaCu_5C_6$, an orange residue [125]. Its complicated crystal structure was solved from X-ray powder diffraction data [135] and is shown in Fig. 19.

The crystal structure of $NaCu_5C_6$ consists of a complicated framework of Cu(I) and C_2^{2-} ions, which are connected by Cu–C and short Cu–Cu bonds. At the intersection of small channels, which run parallel to the a and c axis, sodium reside, which are co-ordinated to ten carbon atoms of five C_2 dumbbells. It is the first ternary alkali metal transition metal acetylide, which crystallises in a structure with a three-dimensional transition metal carbon framework. The composition of $NaCu_5C_6$ is close to Cu_2C_2 ($\equiv CuCu_5C_6$) and one might suspect some structural similarities to the binary copper acetylide, whose crystal structure is still unknown, as it can probably be only synthesised in amorphous forms. But the IR and Raman spectra of $NaCu_5C_6$ and Cu_2C_2 show obvious differences, so that a structural similarity is not very likely [136].

Another interesting compound is $(Na_2[Al_4C])_2$, whose existence was predicted by theoretical calculations [137]. It forms a dimeric structure of two tetracoordinate planar carbon $[CAl_4]^{2-}$ building blocks, which are separated by sodium ions. A successful synthesis of this compound has not been reported up to now.

3.2. Ternary alkaline-earth metal carbides

Several ternary alkaline-earth metal carbides containing a transition metal, a main group metal or a semimetal are known. The first compounds of this composition that were synthesised and structurally characterised are those with a perovskite type structure.

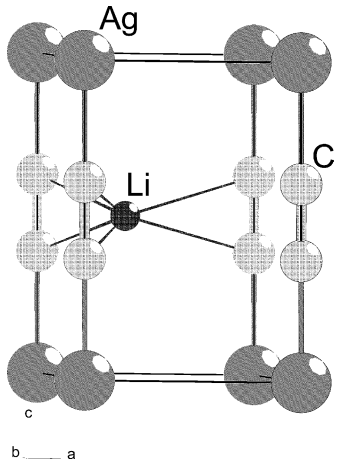

Fig. 16. Crystal structure of $LiAgC_2$ ($P\bar{6}m2$, $Z=1$). The C–C bonds, Ag–C bonds, and the co-ordination of the lithium atom are shown.

$MgNi_3C$ [138], $MgCo_3C$ [139], $MgPt_3C_{1-x}$ [140], and $CaPd_3C$ [141] are described in the literature. The are usually synthesised in typical solid-state reactions by heating the elements. A synthetic route to $MgNi_3C$ from organometallic precursors was also given [142]. In the crystal structures of these carbides $A^{II}M_3C$ (A^{II} alkaline-earth metal; M transition metal) the carbon atoms occupy the octahedral holes of M_6 octahedra. This is shown in Fig. 20.

$MgNi_3C$ is a typical metallic carbide showing an increasing resistivity with increasing temperature. Just recently it has attracted some attention, as it was found to be superconducting at temperatures below 8 K [143]. A partial substitution of Cu (up to 3%) for Ni decreases T_C systematically. Co shows a much higher solubility in $MgNi_3C$, but already small amounts of Co (ca. 1%) suppress superconductivity [144]. A carbon content close to $x=1$ in $MgNi_3C_x$ shows the highest T_C, with smaller x values (up to $x=0.88$) the transition temperature decreases systematically [145].

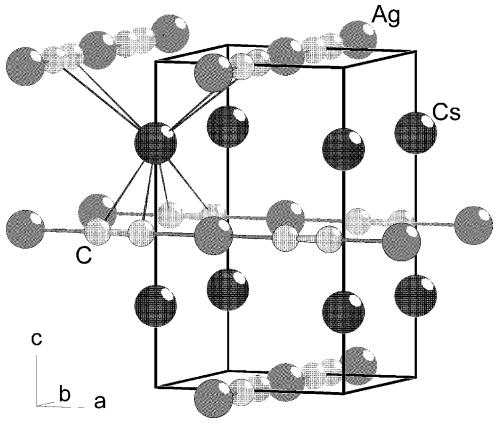

Fig. 17. Crystal structure of $CsAgC_2$ ($P4_2/mmc$, $Z=2$). The C–C bonds, Ag–C bonds, and the co-ordination of one caesium atom are shown.

A magnesium palladium carbide with perovskite type structure has not been reported, only a carbide of composition Mg_2PdC_x is known [146]. It was synthesised from elemental magnesium and palladium in the presence of graphite. The X-ray powder pattern was refined on the basis of a Ti_2Ni structural model for the metal atom substructure, Mg_2Pd. It was not possible to determine the carbon positions in this compound, but other experiments indicated that the carbon content, x, is ≥ 0.1. Because of the unknown carbon structure Mg_2PdC_x will not be discussed in this context any further.

Two modifications of $MgAl_2C_2$ (named T1 and T2) are accessible by reacting graphite particles with Mg–Al melts at 930–1020 K [147]. Below 1000 K a mixture of T1-$MgAl_2C_2$ and T2-$MgAl_2C_2$ is obtained, whereas above 1000 K pure T2-$MgAl_2C_2$ crystallises. Its crystal structure was solved and refined from X-ray powder diffraction data [148]. The structural arrangement is shown in Fig. 21. T2-$MgAl_2C_2$ crystallises in the $CaAl_2Si_2$-type structure. Mg occupies half of the octahedral holes and Al half of the tetrahedral holes of a slightly distorted hexagonal close-packed arrangement of the carbon atoms.

$Ca_4Ni_3C_5$ was prepared from the elemental components by arc melting and subsequent annealing at 770–970 K for several weeks [141]. Thus, single crystals with a metallic lustre and a reddish tint were accessible, which were used to solve the crystal structure of $Ca_4Ni_3C_5$. The resulting atomic arrangement is shown in Fig. 22. The characteristic structural feature is a $_\infty{}^1[Ni_3C_5^{8-}]$ polyanion, which is given in Fig. 23. In this polyanion a single planar carbon atom is co-ordinated by four nickel atoms. Two of the latter are bonded to terminal C_2^{2-} groups (C–C: 120(2) pm), whereas the remaining two

Table 5
Structural data of ternary alkali metal transition metal acetylides of composition AM^IC_2 (A = Li–Cs; M^I = Cu [125], Ag [124], Au [126])

Compound	a (pm)	c (pm)	V (nm^3)	Structure type
$NaCuC_2$	376.61(2)	495.95(2)	0.070343(9)	$KAgC_2$
$KCuC_2$	490.79(3)	762.23(6)	0.18360(3)	$CsAgC_2$
$RbCuC_2$	491.79(8)	832.6(1)	0.20137(9)	$CsAgC_2$
	446.5(1)	492.5(2)	0.09816(6)	$KAgC_2$
$CsCuC_2$	494.06(4)	914.2(1)	0.22314(6)	$CsAgC_2$
$LiAgC_2$	378.82(5)	532.8(3)	0.06621(4)	$LiAgC_2$
$NaAgC_2$	374.7(1)	532.0(1)	0.07469(6)	$KAgC_2$
$KAgC_2$	422.67(8)	528.7(2)	0.09445(6)	$KAgC_2$
$RbAgC_2$	447.5(1)	531.0(1)	0.10634(6)	$KAgC_2$
$CsAgC_2$	524.67(6)	852.8(1)	0.23474(7)	$CsAgC_2$
	471.49(8)	525.9(3)	0.1169(1)	$KAgC_2$
$LiAuC_2$	378.7(5)	519.4(7)	0.0645(3)	$LiAgC_2$
$NaAuC_2$	373.0(8)	520(2)	0.0723(5)	$KAgC_2$
$KAuC_2$	418.4(8)	516(2)	0.0903(6)	$KAgC_2$
$RbAuC_2$	422(2)	519(1)	0.0922(8)	$KAgC_2$
$CsAuC_2$	461(1)	519(1)	0.1101(8)	$KAgC_2$

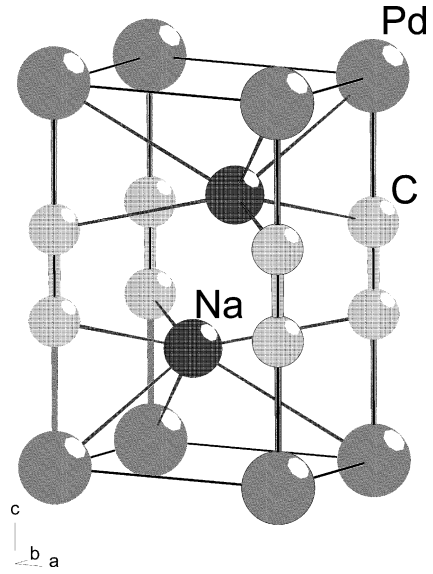

Fig. 18. Crystal structure of Na_2PdC_2 ($P\bar{3}m1$, $Z=1$). The C–C bonds, Pd–C bonds, and the co-ordination of the sodium atoms are shown.

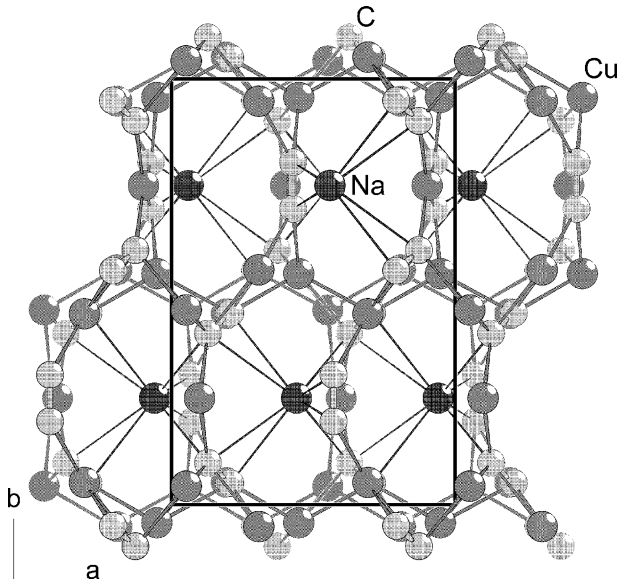

Fig. 19. Crystal structure of $NaCu_5C_6$ (*Pnma*, $Z=4$). The C–C bonds, Cu–C bonds, and the co-ordination of the sodium atoms are shown.

Table 6
Lattice parameters of ternary alkali metal transition metal acetylides of composition A_2MC_2 (A = Na–Cs; M = Pd, Pt) [132,133]

Compound	*a* (pm)	*c* (pm)	*V* (nm^3)
Na_2PdC_2	446.38(1)	526.68(2)	0.090883(7)
K_2PdC_2	510.33(2)	528.28(2)	0.119150(9)
Rb_2PdC_2	535.81(2)	528.88(3)	0.13149(1)
Cs_2PdC_2	562.36(2)	529.76(2)	0.14509(1)
Na_2PtC_2	450.31(3)	520.50(5)	0.09140(1)
K_2PtC_2	512.18(1)	521.79(1)	0.118539(7)
Rb_2PtC_2	536.88(2)	522.45(2)	0.13041(1)
Cs_2PtC_2	563.01(2)	522.94(3)	0.14355(1)

nickel atoms at opposite corners of the square are condensed with further CNi_4 squares to form infinite chains running along the *b* axis of the monoclinic unit cell (see Fig. 22). The linear co-ordination of the nickel atoms points to Ni(0) atoms. Therefore, the following electron count seems to be plausible: $Ca_4^{2+}[Ni_3^0C^{4-}(C_2^{2-})_2]$. Especially, the square planar carbon atom, which is formally a methanide anion, is remarkable. The calcium atoms, which have not been considered in this brief description of the structure, separate the metallorganic nickel–carbon chains. $Ca_4Ni_3C_5$ is diamagnetic with a small negative susceptibility.

To our knowledge neither the synthesis or the crystal structure of a ternary alkali metal or alkaline-earth metal rare earth metal carbide have been reported. Solid solutions were investigated in the system CaC_2–YC_2.

Table 8
Summary of solid-state ^{13}C-MAS-NMR data on ternary alkali metal transition metal acetylides of composition A_2MC_2 [132]

Compound	δ_{iso} [a] (ppm)	$\Delta\sigma$ [b] (ppm)	η [c]
Na_2PdC_2	157	359	0.20
Na_2PtC_2	156	– [d]	– [d]
K_2PdC_2	162	317	0.15
K_2PtC_2	162	– [d]	– [d]

[a] Relative to external tetramethylsilane (TMS) $\delta_{iso} = -\sigma_{iso} = -^1/_3\ 1/3(\sigma_{11}+\sigma_{22}+\sigma_{33})$; $|\sigma_{33}-\sigma_{iso}| \geq |\sigma_{11}-\sigma_{iso}| \geq |\sigma_{22}-\sigma_{iso}|$.
[b] Anisotropy: $\Delta\sigma = \sigma_{33} - 1/2(\sigma_{11}+\sigma_{22})$.
[c] Asymmetry: $\eta = 3/2(\sigma_{22}-\sigma_{11})/\Delta\sigma$.
[d] Not determined.

Table 7
Wave numbers (cm^{-1}) of C–C stretching vibrations ($\tilde{\nu}$ (C≡C)) of ternary alkali metal transition metal acetylides as obtained from Raman spectroscopy

	A_2PdC_2	A_2PtC_2	$ACuC_2$ [125]	$AAgC_2$ [124]	$AAuC_2$ [126]
A = Li				1962	1998
A = Na	1862 [132]	1845 [132]		1965	1997
A = K	1850 [132]	1840 [132]	1959	1963	1997
A = Rb	1842 [133]	1833 [133]	1949	1961	1991
A = Cs	1841 [133]	1835 [133]	1945	1965	1993

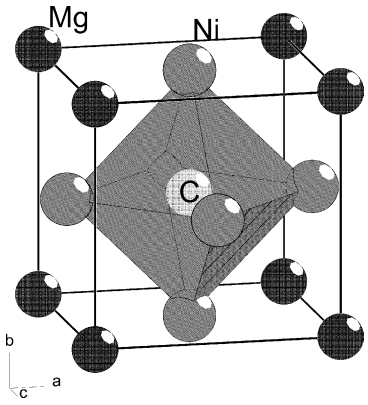

Fig. 20. Crystal structure of $MgNi_3C$ ($Pm\bar{3}m$, $Z=1$). The Ni_6 octahedron centered by a carbon atom is outlined.

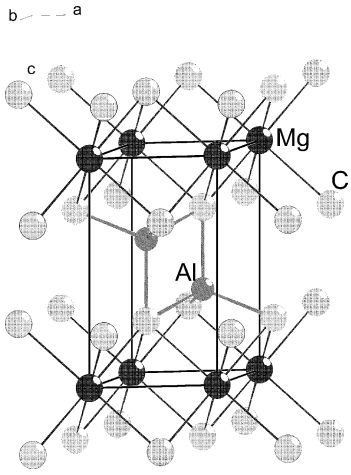

Fig. 21. Crystal structure of TZ-$MgAl_2C_2$ ($P\bar{3}m1$, $Z=1$). The shortest Mg–C and Al–C distances are drawn.

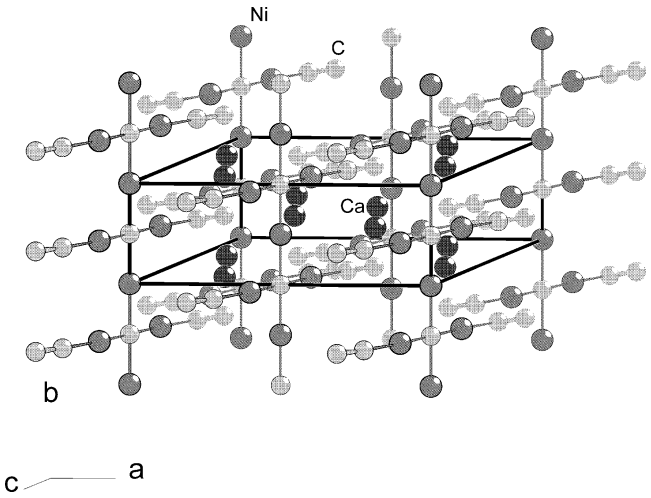

Fig. 22. Crystal structure of $Ca_4Ni_3C_5$ ($C2/m$, $Z=2$). The shortest Ni–C and C–C distances are drawn.

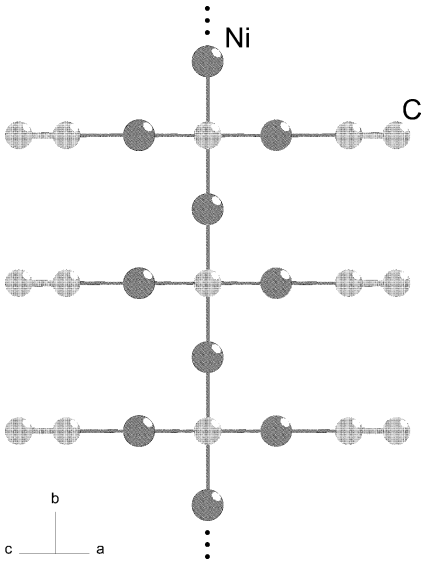

Fig. 23. Part of the one-dimensionally infinite polyanion $^{1}_{\infty}[Ni_3C_5^{8-}]$ in the crystal structure of $Ca_4Ni_3C_5$. The shortest Ni–C and C–C distances are drawn.

Ca^{2+} and Y^{3+} have similar ionic radii and CaC_2 and YC_2 both crystallise in the CaC_2I structure type ($I4/mmm$, $Z=2$). Therefore the system CaC_2–YC_2 was expected to be a good candidate for solid solutions [149]. For the synthesis the pure carbides CaC_2 and YC_2 were heated in different ratios up to 2570 K. And in fact a solubility of Y^{3+} in CaC_2 was proven by different lattice parameters of the solid solutions compared to the pure starting materials and by different hydrolysis products compared to a mixture of CaC_2 and YC_2. It is interesting to note that the hydrolysis of the solid solutions leads to an increase of the released amounts of saturated and unsaturated C_4 hydrocarbons.

A ternary alkaline-earth metal rhenium carbide analogous to Er_2ReC_2 [150] was predicted on the basis of theoretical investigations with extended Hückel calculations. It was found that the states at the *Fermi* level of Er_2ReC_2 have a great deal of Re–C antibonding character, which points to the possible existence of more stable compounds with reduced electron counts. Especially the substitution of Erbium by an alkaline-earth metal should lead to a compound having all the bonding bands filled and all the antibonding bands empty [151]. But a successful synthesis of a carbide of composition $A^{II}_2ReC_2$ (A^{II} alkaline-earth metal) has not been reported up to now.

The only known ternary carbide consisting of an alkaline-earth metal and a semimetal is $Ba_3Ge_4C_2$ [152]. It was synthesised from the elements or by reaction of BaC_2 with $BaGe_2$ at 1530 K. The crystal structure was solved and refined by X-ray single-crystal analysis. The resulting structural arrangement is shown in Fig. 24. It consists of slightly compressed tetrahedral $[Ge_4]^{4-}$ anions inserted in a twisted octahedral $Ba_{6/2}$ 3D frame-

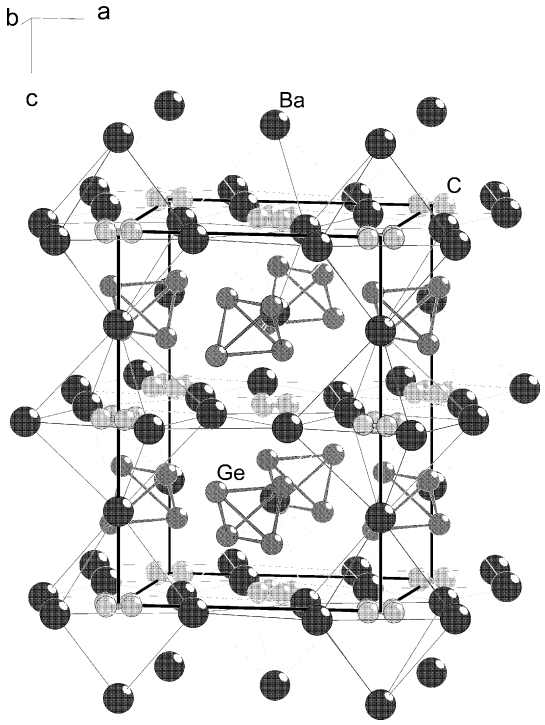

Fig. 24. Crystal structure of $Ba_3Ge_4C_2$ (*I*4/*mcm*, $Z = 4$). The shortest Ba-BA, Ge-Ge, and C-C contacts distances are drawn.

work. The Ba_6 octahedra are centered by C_2^{2-} dumbbells (C–C: 120(6) pm), which are statistically oriented in two directions. The crystal structure can be understood as a cluster-replacement derivative of perovskite: $CaTiO_3 \equiv [Ge_4][C_2]Ba_3$. Pure $Ba_3Ge_4C_2$ is grey, a semiconductor (band gap: 1.1 eV), and the protolysis with NH_4Cl at about 400 K leads to acetylene and germanes up to Ge_4H_n [153]. The Raman spectrum shows a characteristic band for the C–C stretching vibration at 1796 cm^{-1}. This value is significantly smaller than the value found for pure BaC_2 (1831 cm^{-1} [110]). It is possible that a transfer of negative charges from the Ge_4^{4-} tetrahedra to the C_2^{2-} units is responsible for this shift.

4. Conclusion

This overview should show that carbides of Group I and Group II metals are an interesting class of compounds, which were investigated by many research groups over several decades. The research on binary compounds has already started more than 100 years ago, but the development of new methods, mainly the improvements in the field of structure solution from powder diffraction data has led to new research activities, which allowed the answer of several open questions. First examples for ternary carbides of Group I and Group II metals including a transition metal were synthesised in the 50s and the 60s of the last century, but structural investigations on most of these compounds 1–4 have been reported only in the last 5 years. As they display interesting physical properties (e.g. superconductivity in $MgNi_3C$) on the borderline between metallic and ionic behaviour, it can be assumed that research activities in this field will produce more fascinating compounds with interesting properties.

Acknowledgements

I would like to thank my co-workers and colleagues, whose contributions to the field overviewed in this contribution have been cited in the references. My special thanks go to U. Cremer and B. Zibrowius for proof-reading the manuscript and their helpful hints and discussions.

References

[1] S. Windisch, H. Nowotny, Preparation of transition-metal carbides and related compounds, in: P. Hagenmuller (Ed.), Preparation Methods in Solid State Chemistry, Academic Press, New York, 1972, p. 533 ff.
[2] H. Holleck, Binary and Ternary Carbide and Nitride Systems of Transition Metals (in German), Gebrüder Bornträger, Berlin, 1984.
[3] H. Nowotny, Angew. Chem. 84 (1972) 973.
[4] W. Jeitschko, M.H. Gerss, R.D. Hoffmann, S. Lee, J. Less-Common Met. 156 (1989) 397.
[5] R.B. King, Russ. Chem. Bull. 43 (1994) 1285.
[6] R.B. King, J. Organomet. Chem. 536–537 (1997) 7.
[7] (a) A.F. Wells, Structural Inorganic Chemistry, fourth ed., Clarendon Press, Oxford, 1975, p. 756 ff;
(b) H.-J. Meyer, Metallcarbide (in German), in: E. Riedel (Ed.), Moderne Anorganische Chemie, de Gruyter, Berlin, New York, 1999, p. 424 ff.
[8] B. Albert, K. Schmitt, Inorg. Chem. 38 (1999) 6159.
[9] R.J. Cava, H. Takagi, H.W. Zandbergen, J.J. Krajewski, W.F. Peck, Jr., T. Siegrist, R.B. van Dover, R.J. Felder, K. Mizuhashi, J.O. Lee, H. Eisaki, S. Uchida, Nature 367 (1994) 146.
[10] H.-J. Meyer, Z. Anorg. Allg. Chem. 593 (1991) 185.
[11] A. Simon, H. Mattausch, R. Eger, R.K. Kremer, Angew. Chem. 103 (1991) 1210; Angew. Chem. Int. Ed. 30 (1991) 1188.
[12] W. Rüdorff, Graphite intercalation compounds, in: Advances in Inorganic Chemistry and Radiochemistry, 1959, p. 223 ff.
[13] H. Kuzmany, Phys. Unserer Zeit 1 (1998) 16.
[14] E. Weiss, Angew. Chem., 105 (1993) 1565; Angew. Chem. Int. Ed., 32 (1993) 1501.
[15] H. Föppl, Angew. Chem. 70 (1958) 401.
[16] E. Weiss, H. Plass, Chem. Ber. 101 (1968) 2947.
[17] M. Atoji, J. Chem. Phys. 56 (1972) 4947.
[18] R. Nast, Coord. Chem. Rev. 47 (1982) 89.
[19] J.R. Baran, Jr., C. Hendrickson, D.A. Laude, Jr., R.J. Lagow, J. Org. Chem. 57 (1992) 3759.
[20] M. Unno, K. Negishi, H. Matsumoto, Chem. Lett. 4 (2001) 340.
[21] C. Chung, R.J. Lagow, J. Chem. Soc. Chem. Commun. (1972) 1078.
[22] F.J. Landro, J.A. Gurak, J.W. Chinn, Jr., R.J. Lagow, J. Organomet. Chem. 249 (1983) 1.
[23] L.A. Shimp, R.J. Lagow, J. Am. Chem. Soc. 95 (1973) 1343.

[24] L.A. Shimp, J.A. Morrison, J.A. Gurak, J.W. Chinn, Jr., R.J. Lagow, J. Am. Chem. Soc. 103 (1981) 5951.
[25] F.J. Landro, J.A. Gurak, J.W. Chinn, Jr., R.M. Newman, R.J. Lagow, J. Am. Chem. Soc. 104 (1982) 7345.
[26] J.B. Collins, J.D. Dill, E.D. Jemmis, Y. Apeloig, P.v.R. Schleyer, R. Seeger, J.A. Pople, J. Am. Chem. Soc. 98 (1976) 5419.
[27] L.-S. Wang, A.I. Boldyrev, X. Li, J. Simons, J. Am. Chem. Soc. 122 (2000) 7681.
[28] X.E. Zheng, Z.Z. Wang, A.C. Tang, Theochem 492 (1999) 105.
[29] M.H. Moissan, C. R. Acad. Sci. 126 (1898) 302.
[30] M.H. Moissan, C. R. Acad. Sci. 127 (1898) 911.
[31] M.H. Moissan, C. R. Acad. Sci. 136 (1903) 1217.
[32] M.H. Moissan, Bl. Soc. Chim. Fr. 31 (1904) 511.
[33] U. Ruschewitz, W. Kockelmann, Z. Anorg. Allg. Chem. 625 (1999) 1041.
[34] M. Corbellini, L. Turner, Chim. Ind. (Milan) 42 (1960) 251.
[35] O.F. Beumel, Jr., R.F. Harris, J. Org. Chem. 28 (1963) 2775.
[36] U. Ruschewitz, unpublished results.
[37] R. Juza, V. Wehle, H.-U. Schuster, Z. Anorg. Allg. Chem. 352 (1965) 252.
[38] U. Ruschewitz, R. Pöttgen, Z. Anorg, Allg. Chem. 625 (1999) 1599.
[39] M.H. Moissan, C. R. Acad. Sci. 122 (1896) 362.
[40] D.R. Secrist, L.G. Wisnyi, Acta Crystallogr. 15 (1962) 1042.
[41] R. Juza, V. Wehle, Naturwissenschaften 52 (1965) 537.
[42] H. Föppl, Z. Anorg. Allg. Chem. 291 (1957) 12.
[43] L. Pauling, The Nature of the Chemical Bond, third ed., Cornell University Press, Ithaca, 1960.
[44] H. Bärnighausen, Commun. Math. Chem. 9 (1980) 139.
[45] M. Atoji, J. Chem. Phys. 60 (1974) 3324.
[46] S. Hemmersbach, B. Zibrowius, U. Ruschewitz, Z. Anorg. Allg. Chem. 625 (1999) 1440.
[47] U. Ruschewitz, unpublished results.
[48] R.C. Weast, Handbook of Chemistry and Physics, 54th ed., CRC Press, Cleveland, 1973–1974, p. B137.
[49] K.-H. Klöss, D. Hinz-Hübner, U. Ruschewitz, Z. Anorg. Allg. Chem. 628 (2002) 2701.
[50] U. Ruschewitz, P. Müller, W. Kockelmann, Z. Anorg. Allg. Chem. 627 (2001) 513.
[51] B. Winkler, V. Milman, Solid State Commun. 121 (2002) 155.
[52] (a) H. Braekken, Z. Kristallogr. 83 (1932) 222;
(b) K. Sahl, J. Zemann, Naturwissenschaften 48 (1961) 641.
[53] R. Nesper, Habilitationsschrift, MPI Stuttgart (Germany), 1988.
[54] G. Herzberg, Molecular Spectra and Molecular Structure, Vol. I: Spectra of Diatomic Molecules Vol. II: Infrared and Raman Spectra of Polyatomic Molecules, Van Nostrand Reinhold Co, New York, Toronto, London, Melbourne, 1945.
[55] R. Nast, J. Gremm, Z. Anorg. Allg. Chem. 325 (1963) 62.
[56] T.M. Duncan, Inorg. Chem. 28 (1989) 2663.
[57] A.J. Beeler, A.M. Orendt, D.M. Grant, P.W. Cutts, J. Michl, K.W. Zilm, J.W. Downing, J.C. Facelli, M.S. Schindler, W. Kutzelnigg, J. Am. Chem. Soc. 106 (1984) 7672.
[58] R. West, P.A. Carney, I.C. Mineo, J. Am. Chem. Soc. 87 (1965) 3788.
[59] R. West, P.C. Jones, J. Am. Chem. Soc. 91 (1969) 6156.
[60] U. Ruschewitz, unpublished results.
[61] W. Priester, R. West, T.L. Chwang, J. Am. Chem. Soc. 98 (1976) 8413.
[62] (a) E.D. Jemmis, D. Poppinger, P.v.R. Schleyer, J.A. Pople, J. Am. Chem. Soc. 99 (1977) 5796;
(b) D.S. Marynick, C. Hawkins, Organometallics 15 (1996) 882.
[63] (a) H. Kleykamp, J. Nucl. Mat. 294 (2001) 88;
(b) W.-S. Shih, R.B. Stephens, W.J. James, Fusion Technol. 37 (2000) 24.
[64] M. Lebeau, C. R. Acad. Sci. Paris 121 (1895) 496.
[65] C. Fichter, E. Brunner, Z. Anorg. Allg. Chem. 93 (1915) 91.
[66] M. von Stackelberg, F. Quatram, Z. Physik. Chem. 27 (1935) 50.
[67] C.H. Lee, W.R.L. Lambrecht, B. Segall, Phys. Rev. B 51 (1995) 10392.
[68] J.L. Corkill, M.L. Cohen, Phys. Rev. B 48 (1993) 17138.
[69] A.I. Boldyrev, J. Simons, J. Phys. Chem. A 101 (1997) 902.
[70] P. Fuentealba, J. Mol. Struc. 493 (1999) 139.
[71] J.F. Durand, Bull. Soc. Chim. 35 (1924) 1141.
[72] W. Koch, G. Frenking, J. Gauss, D. Cremer, A. Sawaryn, P.v.R. Schleyer, J. Am. Chem. Soc. 108 (1986) 5732.
[73] P. Fuentealba, A. Savin, J. Phys. Chem. A 104 (2000) 10882.
[74] J. Novák, Z. Physik. Chem. 73 (1910) 513.
[75] H.H. Franck, M.A. Bredig, K.-H. Kou, Z. Anorg. Allg. Chem. 232 (1937) 75.
[76] W.H.C. Rueggeberg, J. Am. Chem. Soc. 65 (1943) 602.
[77] F. Irmann, Helv. Chim. Acta 31 (1948) 1584.
[78] A. Schneider, J.F. Cordes, Z. Anorg. Allg. Chem. 279 (1955) 94.
[79] B. Hájek, P. Karen, V. Brozek, Collect. Czech. Chem. Commun. 48 (1983) 1969.
[80] V. Vohn, U. Ruschewitz, Z. Kristallogr. Suppl. 15 (1998) 55.
[81] P. Karen, A. Kjekshus, Q. Huang, V.L. Karen, J. Alloy. Compds. 282 (1999) 72.
[82] E.B. Hunt, R.E. Rundle, J. Am. Chem. Soc. 73 (1951) 4777.
[83] S. Green, Chem. Phys. Lett. 112 (1984) 29.
[84] A.I. Boldyrev, J. Simons, J. Phys. Chem. A 101 (1997) 2215.
[85] C. Winkler, Ber. Dtsch. Chem. Ges. 23 (1890) 2642.
[86] L. Maquenne, C. R. Acad. Sci. 115 (1892) 558.
[87] H. Moissan, C. R. Acad. Sci. 115 (1892) 1031.
[88] H. Moissan, C. R. Acad. Sci. 118 (1894) 684.
[89] H. Moissan, Bl. Soc. Chim. 11 (1894) 1002.
[90] M. von Stackelberg, Naturwissenschaften 18 (1930) 305.
[91] M. von Stackelberg, Z. Physik. Chem. B 9 (1930) 437.
[92] M. Atoji, R.C. Medrud, J. Chem. Phys. 31 (1959) 332.
[93] O. Reckeweg, A. Baumann, H.A. Mayer, J. Glaser, H.-J. Meyer, Z. Anorg. Allg. Chem. 625 (1999) 1686.
[94] H.H. Franck, M.A. Bredig, G. Hoffmann, Z. Anorg. Allg. Chem. 232 (1937) 61.
[95] M.A. Bredig, J. Phys. Chem. 46 (1942) 801.
[96] M. Atoji, J. Chem. Phys. 54 (1971) 3514.
[97] N.-G. Vannerberg, Acta Chem. Scand. 16 (1962) 1212.
[98] M. Knapp, U. Ruschewitz, Chem. Eur. J. 7 (2001) 874.
[99] N.-G. Vannerberg, Acta Chem. Scand. 15 (1961) 769.
[100] J. Glaser, S. Dill, M. Marzini, H.A. Mayer, H.-J. Meyer, Z. Anorg. Allg. Chem. 627 (2001) 1090.
[101] R. Juza, H.-U. Schuster, Z. Anorg. Allg. Chem. 311 (1961) 62.
[102] J.R. Long, R. Hoffmann, H.-J. Meyer, Inorg. Chem. 31 (1992) 1734.
[103] E. Ruiz, P. Alemany, J. Phys. Chem. 99 (1995) 3114.
[104] H. Moissan, Bl. Soc. Chim. 11 (1894) 1007.
[105] H. Moissan, Ann. Chim. Phys. 9 (1896) 247.
[106] V. Vohn, M. Knapp, U. Ruschewitz, J. Solid State Chem. 151 (2000) 111.
[107] H. Moissan, Bl. Soc. Chim. 11 (1894) 1008.
[108] V. Vohn, W. Kockelmann, U. Ruschewitz, J. Alloy. Compd. 284 (1999) 132.
[109] U. Ruschewitz, unpublished results.
[110] P. Pyykkö, J. Mol. Phys. 67 (1989) 871.
[111] B. Zibrowius, U. Ruschewitz, unpublished results.
[112] B. Wrackmeyer, K. Horchler, A. Sebald, L.H. Merwin, C. Ross, Angew. Chem. 102 (1990) 821; Angew Chem. Int. Ed. 29 (1990) 807.
[113] B. Hájek, P. Karen, V. Brozek, Collect. Czech. Chem. Commun. 48 (1983) 1963.
[114] J.F. Cordes, K. Wintersberger, Z. Naturforsch. B 12 (1957) 136.
[115] B. Hájek, P. Karen, V. Brozek, Collect. Czech. Chem. Commun. 45 (1980) 3408.
[116] W.A. Peters, J.B. Howard, MIT, U.S.P.4921685, May 1, 1990.
[117] W.A. Peters, J.B. Howard, MIT, U.S.P.5246550, September 21, 1993.

[118] J.D. Allison, R.M. Tillman, Conoco Inc., U.S.P.4899004, February 6, 1990.
[119] H. Fjellvåg, P. Karen, Inorg. Chem. 31 (1992) 3260.
[120] B.P. Stoicheff, Can. J. Chem. 33 (1955) 811.
[121] R. Pöttgen, W. Jeitschko, Inorg. Chem. 30 (1991) 431.
[122] P. Karen, H. Fjellvåg, J. Alloy. Compds. 178 (1992) 285.
[123] R. Nast, H. Schindel, Z. Anorg. Allg. Chem. 326 (1963) 201.
[124] W. Kockelmann, U. Ruschewitz, Angew. Chem. 111 (1999) 3697; Angew. Chem. Int. Ed. 38 (1999) 3492.
[125] U. Cremer, W. Kockelmann, M. Bertmer, U. Ruschewitz, Solid State Sci. 4 (2002) 247.
[126] J. Offermanns, U. Ruschewitz, C. Kneip, Z. Anorg. Allg. Chem. 626 (2000) 649.
[127] M. O'Keeffe, S. Andersson, Acta Crystallogr. A 33 (1977) 914.
[128] P. Pyykkö, Chem. Rev. 88 (1988) 563.
[129] S. Kroeker, R.E. Wasylishen, J.V. Hanna, J. Am. Chem. Soc. 121 (1999) 1582.
[130] S. Kroeker, R.E. Wasylishen, Can. J. Chem. 77 (1999) 1962.
[131] M. Weiß, U. Ruschewitz, Z. Anorg. Allg. Chem. 623 (1997) 1208.
[132] S. Hemmersbach, B. Zibrowius, W. Kockelmann, U. Ruschewitz, Chem. Eur. J. 7 (2001) 1952.
[133] U. Ruschewitz, Z. Anorg. Allg. Chem. 627 (2001) 1231.
[134] (a) U. Ruschewitz, K.-H. Klöss, C. Bähtz, M. Knapp, Z. Anorg. Allg. Chem. 628 (2002) 2228;
(b) U. Ruschewitz, C. Bähtz, M. Knapp, Z. Anorg. Allg. Chem. 629 (2003) 1581.
[135] U. Cremer, U. Ruschewitz, Z. Anorg. Allg. Chem. 628 (2002) 2207.
[136] U. Cremer, U. Ruschewitz, Z. Anorg. Allg. Chem., accepted.
[137] G.D. Geske, A.I. Boldyrev, Inorg. Chem. 41 (2002) 2795.
[138] E. Scheil, L. Huetter, Z. Metallkd. 44 (1953) 387.
[139] L. Huetter, H. Stadelmaier, Acta Metall. 52 (1958) 367.
[140] H. Stadelmaier, W.K. Hardy, Z. Metallkd. 52 (1961) 391.
[141] U.E. Musanke, W. Jeitschko, Z. Naturforsch. B 46 (1991) 1177.
[142] B. Bogdanovic, K.-H. Claus, S. Gürtzgen, B. Spliethoff, U. Wilczok, J. Less-Common Met. 131 (1987) 163.
[143] T. He, Q. Huang, A.P. Ramirez, Y. Wang, K.A. Regan, N. Rogado, M.A. Hayward, M.K. Haas, J.S. Slusky, K. Inumara, H.W. Zandbergen, N.P. Ong, R.J. Cava, Nature 411 (2001) 54.
[144] M.A. Hayward, M.K. Haas, A.P. Ramirez, T. He, K.A. Regan, N. Rogado, K. Inumaru, R.J. Cava, Solid State Commun. 119 (2001) 491.
[145] T.G. Amos, Q. Huang, J.W. Lynn, T. He, R.J. Cava, Solid State Commun. 121 (2002) 73.
[146] D. Noréus, J. Less-Common Met. 169 (1991) 369.
[147] J.C. Viala, F. Bosselet, G. Claveyrolas, B.F. Mentzen, J. Bouix, Eur. J. Solid State Inorg. Chem. 28 (1991) 1063.
[148] F. Bosselet, B.F. Mentzen, J.C. Viala, M.A. Etoh, J. Bouix, Eur. J. Solid State Inorg. Chem. 35 (1998) 91.
[149] B. Hájek, V. Brozek, M. Popl, Collect. Czech. Chem. Commun. 36 (1971) 1537.
[150] W. Jeitschko, G. Block, G.E. Kahnert, R.K. Behrens, J. Solid State Chem. 89 (1990) 191.
[151] H. Deng, R. Hoffmann, Inorg. Chem. 32 (1993) 1991.
[152] H.G. von Schnering, J. Curda, W. Carrillo-Cabrera, M. Somer, K. Peters, Z. Kristallogr. 211 (1996) 634.
[153] J. Curda, W. Carrillo-Cabrera, A. Schmeding, K. Peters, M. Somer, H.G. von Schnering, Z. Anorg. Allg. Chem. 623 (1997) 929.